

✓ ARL-STRUC-R-446

AR-006-663

2

**AD-A253 448**



**DEPARTMENT OF DEFENCE  
DEFENCE SCIENCE AND TECHNOLOGY ORGANISATION  
AERONAUTICAL RESEARCH LABORATORY**

**MELBOURNE, VICTORIA**

Aircraft Structures Report 446

**STRESSES AND STRAINS IN PLAIN AND COLDWORKED ANNULI  
SUBJECTED TO REMOTE, INTERFERENCE OR COMBINED LOADING**

**S DTIC ELECTE D  
AUG 03 1992  
A**

by

G.S. JOST

This document has been approved for public release and sale; its distribution is unlimited.

Approved for public release

92-20954



© COMMONWEALTH OF AUSTRALIA 1992

MAY 1992

92 8 0 0009

**This work is copyright. Apart from any fair dealing for the purpose of study, research, criticism or review, as permitted under the Copyright Act, no part may be reproduced by any process without written permission. Copyright is the responsibility of the Director Publishing and Marketing, AGPS. Enquiries should be directed to the Manager, AGPS Press, Australian Government Publishing Service, GPO Box 84, CANBERRA ACT 2601.**

**DEPARTMENT OF DEFENCE  
DEFENCE SCIENCE AND TECHNOLOGY ORGANISATION  
AERONAUTICAL RESEARCH LABORATORY**

Aircraft Structures Report 446

**STRESSES AND STRAINS IN PLAIN AND COLDWORKED ANNULI  
SUBJECTED TO REMOTE, INTERFERENCE OR COMBINED LOADING**

by

G.S. JOST

**SUMMARY**

*Analytical plane-strain stresses and strains have been derived for both plain and coldworked annuli subjected to remote loading, interference loading or both loadings acting together. Where required, the deformation theory of plasticity has been used.*

*The comparative influence of the various loading cases on the fatigue process is discussed. Under cyclic remote loading, it is predicted that the most beneficial fatigue situation will result from a combination of interference fitting and coldworking.*



© COMMONWEALTH OF AUSTRALIA 1992

**POSTAL ADDRESS:**

**Director, Aeronautical Research Laboratory  
506 Lorimer Street, Fishermens Bend 3207  
Victoria Australia**

Accession For	
NTIS CRA&I	<input checked="" type="checkbox"/>
DTIC TAB	<input type="checkbox"/>
Unannounced	<input type="checkbox"/>
Justification	
By	
Distribution /	
Availability Codes	
Dist	Avail and/or Special
A-1	

## TABLE OF CONTENTS

	Page Nos.
NOMENCLATURE .....	ii
1. INTRODUCTION .....	1
2. GENERAL RELATIONSHIPS .....	1
2.1 Elastic Region .....	2
2.2 Plastic Region.....	2
3. SOLID PIN WITH REMOTE LOADING .....	3
4. LOADING OF AN UNCOLDWORKED ANNULUS.....	4
4.1 Remote Loading (Open Hole).....	4
4.2 Interference Loading .....	5
4.3 Interference and Remote Loading .....	8
5. COLDWORKED ANNULUS .....	12
5.1 Remote Loading (Open Hole).....	14
5.1.1. Tensile Loading .....	14
5.1.2. Compressive Loading .....	16
5.2 Interference Loading .....	21
5.3 Inteference and Remote Loading .....	23
6. CONCLUSIONS .....	28
REFERENCES.....	28
TABLES 1-8	
FIGURES 1-13	
DISTRIBUTION	
DOCUMENT CONTROL DATA	

NOMENCLATURE

$a$	hole radius
$b$	outer radius of annulus
$c$	elasto-plastic radius resulting from coldworking
$D$	expression defined by equation (24)
$E$	Young's modulus of annulus material
$E_p$	Young's modulus of pin material
$g$	ratio $E/E_p$
$i$	dimensionless interference, $I/a$
$I$	radial interference
$\ln$	natural logarithm
$p$	pressure
$r$	radius
$S$	uniform remote stress applied at radius $b$
$\bar{S}$	mean remote stress applied at radius $b$
$u$	displacement
$\alpha$	radius defined by equation (66)
$\Delta$	range (prefix)
$\epsilon$	strain
$\nu$	Poisson's ratio
$\rho$	reyield radius resulting from recovery after coldworking
$\sigma$	stress
$\bar{\sigma}$	mean stress
$\tau$	reyield radius resulting from compressive remote loading of open coldworked annulus

Subscripts

$a$	at bore
$c$	at elasto-plastic radius
$cw$	coldworking
$o$	yield
$p$	pin
$r$	radial
$z$	axial
$\theta$	circumferential

## 1. INTRODUCTION

The fatigue process in aircraft structures is invariably associated with the presence of stress concentrations of one kind or another, and fastener holes represent by far the most numerous such feature in any metallic structure. Substantial attention has been given to developing methods for improving the fatigue behaviour of structures containing holes, and, in aircraft structural manufacture, interference fitting and hole coldworking are now two of the most common processes used to achieve such improvement. Each technique achieves its beneficial effect by modifying the stress field around the hole to inhibit or delay the onset and progress of fatigue cracking.

The structural feature considered in this report is an annulus, the bore of which may be interference fitted and/or coldworked, and to the perimeter of which remote loading may be applied. In an earlier report<sup>1</sup>, analytical plane-strain stress and strain relationships were derived for an elastic/perfectly-plastic annulus containing a coldworked hole using deformation plasticity theory. A comparison there of the results with those from finite element calculations using incremental plasticity theory<sup>2</sup> showed that the analytical theory gave predictions in good agreement with the more accurate assessments. This being so, it was considered useful to extend the analytical work of the earlier report to include the effect of interference fitting and of remote loading applied around the outer perimeter of the annulus. The conditions leading to the minimising of both stress range and maximum stress at the hole (the usual fatigue-critical location) may then be readily understood.

The cases considered here are listed in Table 1. Stresses and strains in both plain (uncoldworked) and coldworked holes are derived for the cases of interference loading, remote loading and for both loadings acting together, i.e. combined loading. The case of a loaded solid pin is included for completeness. The valid ranges for all solutions are specified, and the values of all parameters used in the numerical examples considered throughout the report are listed in Tables 2(a) and 2(b) respectively.

## 2. GENERAL RELATIONSHIPS

In the axisymmetric problems to be discussed, the radial, circumferential and axial directions are also the principal directions. All formulations are given in terms of these principal directions.

## 2.1 Elastic Region

For plane strain conditions ( $\epsilon_z = 0$ ) the following general relationships hold<sup>3</sup>:

$$\begin{aligned}\epsilon_r &= [\sigma_r - \nu(\sigma_\theta + \sigma_z)] / E = \frac{du_r}{dr} \\ \epsilon_\theta &= [\sigma_\theta - \nu(\sigma_z + \sigma_r)] / E = \frac{u_r}{r} \\ \epsilon_z &= [\sigma_z - \nu(\sigma_r + \sigma_\theta)] / E = 0\end{aligned}\quad (1)$$

From the last of these

$$\sigma_z = \nu(\sigma_r + \sigma_\theta) \quad (2)$$

and back-substitution to eliminate  $\sigma_z$  provides

$$\begin{aligned}\epsilon_r &= \frac{1+\nu}{E} \{(1-\nu)\sigma_r - \nu\sigma_\theta\} \\ \epsilon_\theta &= \frac{1+\nu}{E} \{(1-\nu)\sigma_\theta - \nu\sigma_r\}\end{aligned}\quad (3)$$

From the second of (1), knowledge of circumferential strain alone at radius  $r$  is required to determine radial displacement there:

$$u_r = r\epsilon_\theta \quad (4)$$

## 2.2 Plastic Region

In this report, deformation plasticity theory is used. The following assumptions are made:

- (a) Incompressibility - plastic flow occurs with no change in volume. This corresponds to Poisson's ratio becoming equal to one half.
- (b) Plane strain - as before,  $\epsilon_z = 0$ , and from the Hencky equations it follows that

$$\sigma_z = \frac{1}{2}(\sigma_r + \sigma_\theta) \quad (5)$$

and

$$\epsilon_r + \epsilon_\theta = 0 \quad (6)$$

These results also follow directly from (1) and (2) with  $\nu = 1/2$ .

(c) Yield criterion - in terms of principal stresses, the von Mises criterion is given by

$$(\sigma_r - \sigma_\theta)^2 + (\sigma_\theta - \sigma_z)^2 + (\sigma_z - \sigma_r)^2 = 2\sigma_0^2$$

Substituting for  $\sigma_z$  from (2) gives

$$\sigma_r - \sigma_\theta = \pm \frac{2}{\sqrt{3}}\sigma_0 \quad (7)$$

(d) An elastic/perfectly-plastic stress-strain relationship is assumed in both positive and negative senses. Work hardening does not occur and the Bauschinger effect does not exist.

Because of these simplifications, incompatibilities do occur - in particular, because of the need for step changes in the value of  $\nu$  across elasto-plastic boundaries. For practical purposes, however, these inconsistencies are either small in magnitude or affect quantities of secondary interest only.

### 3. SOLID PIN WITH REMOTE LOADING

A uniform stress  $S$  applied to the outer boundary of a solid pin, Fig. 1(a), gives rise to particularly simple elastic stress distributions<sup>3</sup>:

$$\sigma_{rp} = \sigma_{\theta p} = S \quad (8)$$

Substitution of (8) into (3) provides the corresponding strains as

$$\epsilon_{rp} = \epsilon_{\theta p} = \frac{S}{E_p}(1 + \nu_p)(1 - 2\nu_p) \quad (9)$$

Thus, both stresses and strains in a uniformly stressed pin in plane strain are everywhere constant and independent of radius.

The above apply equally to the case of external pressure  $p$  acting on the pin, this case simulating the loading seen by an interference-fitted pin in a hole. In this case  $S$  is replaced by  $-p$ .

Under conditions of plane strain, yielding of a pin cannot take place. The yield equation (7) cannot be satisfied by (8). Thus in all situations involving interference fitting, irrespective of the behaviour of the plate, the pin remains elastic.

#### 4. LOADING OF AN UNCOLDWORKED ANNULUS

In this Section the stresses and strains in an uncoldworked annulus resulting from remote loading, interference loading and both loadings acting together are examined. The effect of cyclic remote loading is also evaluated.

##### 4.1 Remote Loading (Open Hole)

The stresses for this case, Fig. 1(b), are given by<sup>3</sup>

$$\begin{aligned}\sigma_r &= S \frac{1 - \left(\frac{a}{r}\right)^2}{1 - \left(\frac{a}{b}\right)^2} \\ \sigma_\theta &= S \frac{1 + \left(\frac{a}{r}\right)^2}{1 - \left(\frac{a}{b}\right)^2}\end{aligned}\quad (10)$$

Under cyclic loading these become

$$\begin{aligned}\Delta\sigma_r &= \Delta S \frac{1 - \left(\frac{a}{r}\right)^2}{1 - \left(\frac{a}{b}\right)^2} \\ \Delta\sigma_\theta &= \Delta S \frac{1 + \left(\frac{a}{r}\right)^2}{1 - \left(\frac{a}{b}\right)^2}\end{aligned}\quad (11)$$

The circumferential cyclic stress range is a maximum at the bore, being given by

$$\left(\frac{\Delta\sigma_\theta}{\Delta S}\right)_a = \frac{2}{1 - \left(\frac{a}{b}\right)^2}\quad (12)$$

Comparison of  $\sigma_\theta$  from (10) with its solid pin equivalent at (8) shows the stress concentrating effect of the open hole represented by the factor following  $S$  in (10). When the annulus is large, this factor approaches the familiar 2.0 for an infinite plate under biaxial loading.

Increase in  $S$  eventually leads to the onset of plastic flow at the bore. Substitution of (10) into the yield criterion (7), and setting  $r = a$  gives the value of applied stress to initiate yield there as

$$S_o = \pm \frac{\sigma_o}{\sqrt{3}} \left[ 1 - \left(\frac{a}{b}\right)^2 \right]\quad (13)$$

at which stage

$$\begin{aligned}\sigma_{r0} &= \pm \frac{\sigma_0}{\sqrt{3}} \left[ 1 - \left( \frac{a}{r} \right)^2 \right] \\ \sigma_{\theta 0} &= \pm \frac{\sigma_0}{\sqrt{3}} \left[ 1 + \left( \frac{a}{r} \right)^2 \right]\end{aligned}\quad (14)$$

The elastic strains are readily found from (10) and (3) as

$$\begin{aligned}\epsilon_r &= -\frac{S}{E} \left[ \frac{1+\nu}{1-\left(\frac{a}{b}\right)^2} \right] \left[ \left( \frac{a}{r} \right)^2 - (1-2\nu) \right] \\ \epsilon_\theta &= \frac{S}{E} \left[ \frac{1+\nu}{1-\left(\frac{a}{b}\right)^2} \right] \left[ \left( \frac{a}{r} \right)^2 + (1-2\nu) \right]\end{aligned}\quad (15)$$

Substitution for  $S_0$  from (13) for  $S$  in (15) gives the strains at radius  $r$  corresponding to the onset of yield at radius  $a$  as (with  $\nu = 1/2$ )

$$\begin{aligned}\epsilon_{r0} &= \mp \frac{\sqrt{3} \sigma_0}{2 E} \left( \frac{a}{r} \right)^2 \\ \epsilon_{\theta 0} &= \pm \frac{\sqrt{3} \sigma_0}{2 E} \left( \frac{a}{r} \right)^2\end{aligned}\quad (16)$$

Thus, checks on whether the yield point has been reached at the bore may be found from (13) in terms of applied stress or from (16) in terms of strain measured at radius  $r$ .

#### 4.2 Interference Loading

The interference fitting of a pin into the hole, Fig. 1(c), generates an interface pressure which gives rise to radial displacements of both pin and annulus such that

$$I = u_a - u_{ap}$$

or

$$i = \frac{I}{a} = \frac{u_a}{a} - \frac{u_{ap}}{a} = (\epsilon_\theta)_a - (\epsilon_{\theta p})_a \quad (17)$$

Since the surface displacement of the pin,  $u_{ap}$ , is always negative (i.e. towards its centre), (17) is always positive.

The stresses in an internally pressurised annulus are given by<sup>3</sup>

$$\begin{aligned}\sigma_r &= -p \frac{\left(\frac{a}{r}\right)^2 - \left(\frac{a}{b}\right)^2}{1 - \left(\frac{a}{b}\right)^2} \\ \sigma_\theta &= p \frac{\left(\frac{a}{r}\right)^2 + \left(\frac{a}{b}\right)^2}{1 - \left(\frac{a}{b}\right)^2}\end{aligned}\quad (18)$$

and those for an externally pressurised pin (8) by

$$\sigma_{rp} = \sigma_{\theta p} = -p \quad (19)$$

The corresponding strains are given by

$$\begin{aligned}\epsilon_r &= -\frac{p}{E} \left[ \frac{1+\nu}{1 - \left(\frac{a}{b}\right)^2} \right] \left[ \left(\frac{a}{r}\right)^2 - (1-2\nu) \left(\frac{a}{b}\right)^2 \right] \\ \epsilon_\theta &= \frac{p}{E} \left[ \frac{1+\nu}{1 - \left(\frac{a}{b}\right)^2} \right] \left[ \left(\frac{a}{r}\right)^2 + (1-2\nu) \left(\frac{a}{b}\right)^2 \right]\end{aligned}\quad (20)$$

and, from (9),

$$\epsilon_{rp} = \epsilon_{\theta p} = -\frac{p}{E} (1 + \nu_p) (1 - 2\nu_p) \quad (21)$$

Recalling (4), and setting  $r = a$  there and in (20), provides the radial displacement of the bore of the hole. Equation (4) combined with (21) provides the surface displacement of the pin.

$$\begin{aligned}\frac{u_a}{a} &= \frac{p}{E} (1 + \nu) \frac{1 + (1 - 2\nu) \left(\frac{a}{b}\right)^2}{1 - \left(\frac{a}{b}\right)^2} \\ \frac{u_{ap}}{a} &= -\frac{p}{E} (1 + \nu_p) (1 - 2\nu_p)\end{aligned}\quad (22)$$

Substitution of (22) into (17) provides the relationship between interface pressure and interference as

$$\frac{p}{E} = \frac{i \left[ 1 - \left(\frac{a}{b}\right)^2 \right]}{D} \quad (23)$$

where

$$D = (1 + \nu) \left[ 1 + (1 - 2\nu) \left( \frac{a}{b} \right)^2 \right] + g(1 + \nu_p)(1 - 2\nu_p) \left[ 1 - \left( \frac{a}{b} \right)^2 \right] \quad (24)$$

and  $g = E/E_p$ . Figure 2 shows  $D$  as a function of geometry and modulus ratio for the case  $\nu = \nu_p = 1/3$ . In practice, since  $a/b$  is unlikely to exceed 0.5,  $g$  has the more substantial effect. When  $\nu = \nu_p$  and  $g = 1$ ,  $D$  becomes independent of  $a/b$ , being given by

$$D = 2(1 - \nu^2) \quad (25)$$

Substitution of (23) into (18) gives the stresses generated in an annulus by interference loading:

$$\begin{aligned} \sigma_r &= -\frac{iE}{D} \left[ \left( \frac{a}{r} \right)^2 - \left( \frac{a}{b} \right)^2 \right] \\ \sigma_\theta &= \frac{iE}{D} \left[ \left( \frac{a}{r} \right)^2 + \left( \frac{a}{b} \right)^2 \right] \end{aligned} \quad (26)$$

The corresponding strains are given, from (20) and (23), by

$$\begin{aligned} \epsilon_r &= -\frac{i}{D} (1 + \nu) \left[ \left( \frac{a}{r} \right)^2 - (1 - 2\nu) \left( \frac{a}{b} \right)^2 \right] \\ \epsilon_\theta &= \frac{i}{D} (1 + \nu) \left[ \left( \frac{a}{r} \right)^2 + (1 - 2\nu) \left( \frac{a}{b} \right)^2 \right] \end{aligned} \quad (27)$$

Increasing interference leads to the initiation of yield at the bore of the annulus. This point is reached when

$$p_o = \frac{\sigma_o}{\sqrt{3}} \left[ 1 - \left( \frac{a}{b} \right)^2 \right] \quad (28)$$

This is identical to the case of remote loading, (13). In terms of interference, from (23),

$$i_o = \frac{\sigma_o}{\sqrt{3}} \frac{D}{E} \quad (29)$$

As previously noted, plane strain yielding of the pin is impossible.

### 4.3 Interference and Remote Loading

The stresses for this case are found by the superposition of those of the preceding two cases. They are

$$\begin{aligned}\sigma_r &= -p \frac{\left(\frac{a}{r}\right)^2 - \left(\frac{a}{b}\right)^2}{1 - \left(\frac{a}{b}\right)^2} + S \frac{1 - \left(\frac{a}{r}\right)^2}{1 - \left(\frac{a}{b}\right)^2} \\ \sigma_\theta &= p \frac{\left(\frac{a}{r}\right)^2 + \left(\frac{a}{b}\right)^2}{1 - \left(\frac{a}{b}\right)^2} + S \frac{1 + \left(\frac{a}{r}\right)^2}{1 - \left(\frac{a}{b}\right)^2}\end{aligned}\quad (30)$$

The displacement at the bore is written down immediately from (22) and (15) as

$$\frac{u_a}{a} = \frac{p}{E} (1 + \nu) \left[ \frac{1 + (1 - 2\nu) \left(\frac{a}{b}\right)^2}{1 - \left(\frac{a}{b}\right)^2} \right] + \frac{S}{E} \left[ \frac{2(1 - \nu^2)}{1 - \left(\frac{a}{b}\right)^2} \right] \quad (31)$$

and from (22), for the pin,

$$\frac{u_{ap}}{a} = -\frac{p}{E_p} (1 + \nu_p)(1 - 2\nu_p) \quad (32)$$

By introducing the non-dimensional interference  $i$  as before, (17), and substituting (31) and (32) into (17) for this case, the following relationship between  $p$ ,  $S$  and  $i$  is found

$$\frac{p}{E} = \frac{i \left[ 1 - \left(\frac{a}{b}\right)^2 \right] - \frac{S}{E} 2(1 - \nu^2)}{D} \quad (33)$$

where  $D$  is given, as before, by (24).

It can be seen from (33) that, under the action of a sufficiently high tensile  $S$ , separation between pin and hole will occur. From (33), this point is reached when  $p = 0$ , or

$$\frac{S_{sep}}{E} = \frac{i \left[ 1 - \left(\frac{a}{b}\right)^2 \right]}{2(1 - \nu^2)} \quad (34)$$

Interestingly, (34) shows that  $S_{sep}$  is independent of the properties of the pin. For  $S > S_{sep}$  all interference has been lost and conditions are fully described by those of Section 4.1.

By substituting from (33) for  $p$ , stresses (30) may be expressed in terms of interference and remote loading only. They are given by

$$\begin{aligned}\sigma_r &= -\frac{iE}{D} \left[ \left(\frac{a}{r}\right)^2 - \left(\frac{a}{b}\right)^2 \right] + S \frac{1 - \left(\frac{a}{r}\right)^2}{1 - \left(\frac{a}{b}\right)^2} \left\{ 1 + \frac{2(1 - \nu^2)}{D} \left[ \frac{\left(\frac{a}{r}\right)^2 - \left(\frac{a}{b}\right)^2}{1 - \left(\frac{a}{r}\right)^2} \right] \right\} \\ \sigma_\theta &= \frac{iE}{D} \left[ \left(\frac{a}{r}\right)^2 + \left(\frac{a}{b}\right)^2 \right] + S \frac{1 + \left(\frac{a}{r}\right)^2}{1 - \left(\frac{a}{b}\right)^2} \left\{ 1 - \frac{2(1 - \nu^2)}{D} \left[ \frac{\left(\frac{a}{r}\right)^2 + \left(\frac{a}{b}\right)^2}{1 + \left(\frac{a}{r}\right)^2} \right] \right\}\end{aligned}\quad (35)$$

Comparison of (35) with (10) for remote loading alone shows that the second factor in (35) represents the change to the stress field in the annulus effected by interference fitting.

The second of (35) can now be used to establish the circumferential stress range under cyclic loading. The explicit interference term in (35) vanishes leaving

$$\Delta\sigma_\theta = \Delta S \frac{1 + \left(\frac{a}{r}\right)^2}{1 - \left(\frac{a}{b}\right)^2} \left\{ 1 - \frac{2(1 - \nu^2)}{D} \left[ \frac{\left(\frac{a}{r}\right)^2 + \left(\frac{a}{b}\right)^2}{1 + \left(\frac{a}{r}\right)^2} \right] \right\} \quad (36)$$

By multiplying out (36) and rearranging the numerator as

$$2(1 - \nu^2) \left[ 1 - \left(\frac{a}{b}\right)^2 \right] - [2(1 - \nu^2) - D] \left[ 1 + \left(\frac{a}{r}\right)^2 \right] \quad (37)$$

which is of the form  $A - B/r^2$ , it is clear that, provided  $B$  is positive, i.e.  $D < 2(1 - \nu^2)$ , and this will usually be the case, Fig. 2, the magnitude of (37) and hence (36) is a minimum at the bore. This well-known<sup>4</sup>, but nevertheless remarkable, effect derives directly from the interference between pin and hole.

In general terms, the sign of the second term in (37) depends upon the magnitude of  $D$ , which in turn is a monotonic function of  $g$ , the ratio of Young's moduli of annulus to pin, Fig. 2. When the Poisson's ratios for pin and annulus are the same, the second term is positive for  $g < 1$ , and so the magnitude of  $\Delta\sigma_\theta$  decreases towards the bore. When  $g = 1$ ,  $D = 2(1 - \nu^2)$ , the second term vanishes and  $\Delta\sigma_\theta = \Delta S$  and is constant across the section. When  $g > 1$ , the sign of the second term changes and the magnitude of  $\Delta\sigma_\theta$  increases towards the bore. Thus, in order to obtain the maximum possible benefit from interference in a fatigue situation,  $g$  should be as small as possible, i.e. Young's modulus for the pin should be as high as possible and under no circumstances less than that of the annulus material. These behaviours may be seen in Fig. 3 where the cyclic stress range (36) is plotted as a function of  $r/a$  and  $g$  for the case  $b/a = 5$ , assuming  $\nu = \nu_p = 1/3$ . In addition to the behaviour described above, it is seen that the effect of interference fitting is, for  $g < 1$ , to lower the circumferential stress range throughout.

At the bore

$$\left(\frac{\Delta\sigma_\theta}{\Delta S}\right)_a = \frac{2}{1 - \left(\frac{a}{b}\right)^2} \left\{ 1 - \frac{1 - \nu^2}{D} \left[ 1 + \left(\frac{a}{b}\right)^2 \right] \right\} \quad (38)$$

and Fig. 4 shows the effect of changes in geometry and  $g$  (i.e.  $D$ ) on circumferential stress range there.

Comparison of (38) with its counterpart for remote loading of an open annulus (12) shows that the second factor in the braces of (38) represents the benefit gained from interference fitting. The larger this term, the better and, as discussed above, the only means available for effecting this in a given situation is to minimise  $D$ , i.e.  $g$ . Figure 5 shows a comparison of these cases for  $b/a = 5$ . The reduction in circumferential stress range when interference is present, compared with the open hole case, is substantial.

From (35), the mean circumferential stress under cyclic loading is given by

$$\bar{\sigma}_\theta = \frac{iE}{D} \left[ \left(\frac{a}{r}\right) + \left(\frac{a}{b}\right)^2 \right] + \bar{S} \frac{1 + \left(\frac{a}{r}\right)^2}{1 - \left(\frac{a}{b}\right)^2} \left\{ 1 - \frac{2(1 - \nu^2)}{D} \left[ \frac{\left(\frac{a}{r}\right)^2 + \left(\frac{a}{b}\right)^2}{1 + \left(\frac{a}{r}\right)^2} \right] \right\} \quad (39)$$

where the first term and the negative term are the explicit and implicit terms resulting from interference fitting. Clearly, if the second term in braces above were to exceed the first, a net benefit, i.e. reduction, in mean stress would result. Equating those terms gives

$$\bar{S} = iE \frac{1 - \left(\frac{a}{b}\right)^2}{2(1 - \nu^2)} \quad (40)$$

and leaves

$$\bar{\sigma}_\theta = \bar{S} \frac{1 + \left(\frac{a}{r}\right)^2}{1 - \left(\frac{a}{b}\right)^2} \quad (41)$$

Comparison of (40) with (34) shows that  $\bar{S}$  has become equal to  $S_{sep}$ , i.e. all interference has been lost, and the situation is described by (41) = (10). For lower  $S$ , the first term in (39) dominates and the mean circumferential stress throughout is thus always greater than that for the open hole case (41). The mean stress is a maximum at the bore, where

$$(\bar{\sigma}_\theta)_a = \frac{iE}{D} \left[ 1 + \left(\frac{a}{b}\right)^2 \right] + \frac{2\bar{S}}{1 - \left(\frac{a}{b}\right)^2} \left\{ 1 - \frac{1 - \nu^2}{D} \left[ 1 + \left(\frac{a}{b}\right)^2 \right] \right\} \quad (42)$$

Thus, the overall effect of interference fitting is to increase the mean circumferential stress level, (39) and (42), but to decrease the circumferential stress range, (36) and (38). Since the fatigue process is much more sensitive to stress range than to mean stress level, the net result of interference fitting is to increase fatigue life. It is clear that if some means were available to lower the mean stress level whilst retaining the beneficial effect on stress range of interference fitting, the expectation would be for even greater fatigue life. Hole coldworking provides one means of achieving this requirement, and is considered in Section 5.

Strains for the case of interference fitting and remote loading acting simultaneously may be written down directly by superposition from (15) and (20). After substituting from (33) for  $p$  in (20), the results are

$$\begin{aligned} \epsilon_r &= -\frac{i}{D} (1 + \nu) \left[ \left(\frac{a}{r}\right)^2 - (1 - 2\nu) \left(\frac{a}{b}\right)^2 \right] - \frac{S}{E} \left[ \frac{1 + \nu}{1 - \left(\frac{a}{b}\right)^2} \right] \left[ \left(\frac{a}{r}\right)^2 - (1 - 2\nu) \right] \\ &\quad \times \left\{ 1 - \frac{2(1 - \nu^2)}{D} \frac{\left[ \left(\frac{a}{r}\right)^2 - (1 - 2\nu) \left(\frac{a}{b}\right)^2 \right]}{\left[ \left(\frac{a}{r}\right)^2 - (1 - 2\nu) \right]} \right\} \\ \epsilon_\theta &= \frac{i}{D} (1 + \nu) \left[ \left(\frac{a}{r}\right)^2 + (1 - 2\nu) \left(\frac{a}{b}\right)^2 \right] + \frac{S}{E} \left[ \frac{1 + \nu}{1 - \left(\frac{a}{b}\right)^2} \right] \left[ \left(\frac{a}{r}\right)^2 + (1 - 2\nu) \right] \\ &\quad \times \left\{ 1 - \frac{2(1 - \nu^2)}{D} \frac{\left[ \left(\frac{a}{r}\right)^2 + (1 - 2\nu) \left(\frac{a}{b}\right)^2 \right]}{\left[ \left(\frac{a}{r}\right)^2 + (1 - 2\nu) \right]} \right\} \end{aligned} \quad (43)$$

As for stresses, cyclic strain range is found from (43) simply by omitting the interference term and replacing  $S$  by  $\Delta S$ .

For convenience, all (elastic) stresses and strains in the loaded annulus considered in Section 4 have been grouped together in Tables 3 and 4. This allows a ready comparison between the results for differing loading cases to be made. Similarly, Tables 5 and 6 provide similar information for circumferential cyclic stresses and strains.

Finally, it is noted that the onset of yield at the bore for the present case of combined remote loading and interference may be found by substituting from (35) into (7) and setting  $r = a$ . The results are

$$S_o = \pm \frac{\sigma_o}{\sqrt{3}} \left[ 1 - \left(\frac{a}{b}\right)^2 \right] \left\{ \frac{1 \pm \frac{\sqrt{3} i E}{\sigma_o D}}{\frac{2(1 - \nu^2)}{D} - 1} \right\} \quad (44)$$

or

$$i_o = \frac{\sigma_o D}{\sqrt{3} E} \left\{ \mp 1 + \frac{S}{\sigma_o} \frac{\sqrt{3}}{\left[1 - \left(\frac{a}{b}\right)^2\right]} \left[ \frac{2(1 - \nu^2)}{D} - 1 \right] \right\}, \quad S \geq 0 \quad (45)$$

Figure 7 shows the bounds within which the elastic results of Section 4 are valid for the example cases previously considered. The application of high positive remote stress results in separation of the annulus from the pin, (34): yielding of the resulting open hole annulus (13) provides the positive stress limit of elastic behaviour shown. Separation, open hole yield and combined loading cases coincide at the point shown: this can be verified by reference to (34), (13) and (44) respectively. The coordinates of this point are given by

$$\frac{S_o}{\sigma_o} = \frac{1}{\sqrt{3}} \left[ 1 - \left(\frac{a}{b}\right)^2 \right]$$

and

$$i_o = \frac{2}{\sqrt{3}} \frac{\sigma_o}{E} (1 - \nu^2)$$

(46)

## 5. COLDWORKED ANNULUS

The plane strain stresses and strains in a coldworked annulus which has been cold-expanded to cause plastic flow to radius  $c$ , and which has reyielded on unloading to radius  $\rho$ , Fig. 8, are given below<sup>1</sup>.

For the zone  $a \leq r \leq \rho$

$$\begin{aligned} \sigma_r &= -\frac{2\sigma_o}{\sqrt{3}} \ln \frac{r}{a} \\ \sigma_\theta &= -\frac{2\sigma_o}{\sqrt{3}} \left[ 1 + \ln \frac{r}{a} \right] \end{aligned} \quad (47)$$

For the zone  $\rho \leq r \leq c$

$$\begin{aligned} \sigma_r &= \frac{\sigma_o}{\sqrt{3}} \left\{ \left[ 2 \ln \frac{r}{c} - 1 + \left(\frac{c}{b}\right)^2 \right] + 2 \left[ \left(\frac{\rho}{r}\right)^2 - \left(\frac{\rho}{b}\right)^2 \right] \right\} \\ \sigma_\theta &= \frac{\sigma_o}{\sqrt{3}} \left\{ \left[ 2 \ln \frac{r}{c} + 1 + \left(\frac{c}{b}\right)^2 \right] - 2 \left[ \left(\frac{\rho}{r}\right)^2 + \left(\frac{\rho}{b}\right)^2 \right] \right\} \end{aligned} \quad (48)$$

For the zone  $c \leq r \leq b$

$$\begin{aligned}\sigma_r &= \frac{\sigma_o}{\sqrt{3}} \left\{ \left[ -\left(\frac{c}{r}\right)^2 + \left(\frac{c}{b}\right)^2 \right] + 2 \left[ \left(\frac{\rho}{r}\right)^2 - \left(\frac{\rho}{b}\right)^2 \right] \right\} \\ \sigma_\theta &= \frac{\sigma_o}{\sqrt{3}} \left\{ \left[ \left(\frac{c}{r}\right)^2 + \left(\frac{c}{b}\right)^2 \right] - 2 \left[ \left(\frac{\rho}{r}\right)^2 + \left(\frac{\rho}{b}\right)^2 \right] \right\}\end{aligned}\quad (49)$$

The strains in these regions are given by

For the zone  $a \leq r \leq \rho$

$$\begin{aligned}\epsilon_r &= -\frac{(1+\nu)\sigma_o}{\sqrt{3}E} \left\{ \left(\frac{c}{r}\right)^2 \left[ 1 + (1-2\nu)\left(\frac{c}{b}\right)^2 \right] - 2\left(\frac{\rho}{r}\right)^2 \left[ 1 + (1-2\nu)\left(\frac{\rho}{b}\right)^2 \right] \right\} \\ \epsilon_\theta &= -\epsilon_r\end{aligned}\quad (50)$$

For the zone  $\rho \leq r \leq c$

$$\begin{aligned}\epsilon_r &= -\frac{(1+\nu)\sigma_o}{\sqrt{3}E} \left\{ \left(\frac{c}{r}\right)^2 \left[ 1 + (1-2\nu)\left(\frac{c}{b}\right)^2 \right] - 2 \left[ \left(\frac{\rho}{r}\right)^2 - (1-2\nu)\left(\frac{\rho}{b}\right)^2 \right] \right\} \\ \epsilon_\theta &= \frac{(1+\nu)\sigma_o}{\sqrt{3}E} \left\{ \left(\frac{c}{r}\right)^2 \left[ 1 + (1-2\nu)\left(\frac{c}{b}\right)^2 \right] - 2 \left[ \left(\frac{\rho}{r}\right)^2 + (1-2\nu)\left(\frac{\rho}{b}\right)^2 \right] \right\}\end{aligned}\quad (51)$$

For the zone  $c \leq r \leq b$

$$\begin{aligned}\epsilon_r &= -\frac{(1+\nu)\sigma_o}{\sqrt{3}E} \left\{ \left[ \left(\frac{c}{r}\right)^2 - (1-2\nu)\left(\frac{c}{b}\right)^2 \right] - 2 \left[ \left(\frac{\rho}{r}\right)^2 - (1-2\nu)\left(\frac{\rho}{b}\right)^2 \right] \right\} \\ \epsilon_\theta &= \frac{(1+\nu)\sigma_o}{\sqrt{3}E} \left\{ \left[ \left(\frac{c}{r}\right)^2 + (1-2\nu)\left(\frac{c}{b}\right)^2 \right] - 2 \left[ \left(\frac{\rho}{r}\right)^2 + (1-2\nu)\left(\frac{\rho}{b}\right)^2 \right] \right\}\end{aligned}\quad (52)$$

The elasto-plastic radii  $c$  and  $\rho$  in the above are found from

$$\begin{aligned}i_{cw} \frac{E}{\sigma_o} &= \frac{1}{\sqrt{3}} \left\{ (1+\nu) \left(\frac{c}{a}\right)^2 \left[ 1 + (1-2\nu)\left(\frac{c}{b}\right)^2 \right] \right. \\ &\quad \left. + (1+\nu_p)(1-2\nu_p)g \left[ 2\ln\frac{c}{a} + 1 - \left(\frac{c}{a}\right)^2 \right] \right\}\end{aligned}\quad (53)$$

where  $i_{cw}$  is the dimensionless interference used in the coldworking of the annulus and

$$2 \ln \frac{ac}{\rho^2} + 1 - \left(\frac{c}{b}\right)^2 = 2 \left[1 - \left(\frac{\rho}{b}\right)^2\right] \quad (54)$$

These expressions are now used in conjunction with the effects of combined loadings to establish stresses and strains in loaded coldworked annuli.

Figures 9 and 10 show the stress and strain profiles through a coldworked annulus where  $b/a = 5$  and  $c/a = 2.5$ . The locations of the yield ( $c/a = 2.5$ ) and reyield ( $\rho/a = 1.19$ ) boundaries are clear from the circumferential stress plot of Fig. 9. The discontinuities at the same locations visible in the radial strain plot of Fig. 10 are a consequence of the deformation theory of plasticity, whereby the value of Poisson's ratio is required to change abruptly across elasto-plastic boundaries. The effect need manifest itself in only one strain formulation: since radial displacement is a function of circumferential strain (4) (and circumferential displacement is, by symmetry, zero), the correct circumferential strain formulation has been retained here.

### 5.1 Remote Loading (open hole)

The effect of remote loading upon the stress field in a coldworked annulus differs fundamentally, according to whether the loading is tensile or compressive. In the case of tensile loading, superposition of the tensile stress field over that resulting from coldworking is all that is required. Under compressive remote loading, additional yielding occurs near the hole to extend the reyielded region (developed during unloading from cold-expansion) still further. This, in turn, modifies the elastic stress field beyond.

#### 5.1.1 Tensile Loading ( $S > 0$ )

The stresses may be written down directly by superposition from (47) to (49) and (10).

For the zone  $a \leq r \leq \rho$

$$\begin{aligned} \sigma_r &= -\frac{2\sigma_0}{\sqrt{3}} \ln \frac{r}{a} + S \frac{1 - \left(\frac{a}{r}\right)^2}{1 - \left(\frac{a}{b}\right)^2} \\ \sigma_\theta &= -\frac{2\sigma_0}{\sqrt{3}} \left[1 + \ln \frac{r}{a}\right] + S \frac{1 + \left(\frac{a}{r}\right)^2}{1 - \left(\frac{a}{b}\right)^2} \end{aligned} \quad (55)$$

For the zone  $\rho \leq r \leq c$

$$\begin{aligned}\sigma_r &= \frac{\sigma_o}{\sqrt{3}} \left\{ \left[ 2 \ln \frac{r}{c} - 1 + \left( \frac{c}{b} \right)^2 \right] + 2 \left[ \left( \frac{\rho}{r} \right)^2 - \left( \frac{\rho}{b} \right)^2 \right] \right\} + S \frac{1 - \left( \frac{a}{r} \right)^2}{1 - \left( \frac{a}{b} \right)^2} \\ \sigma_\theta &= \frac{\sigma_o}{\sqrt{3}} \left\{ \left[ 2 \ln \frac{r}{c} + 1 + \left( \frac{c}{b} \right)^2 \right] - 2 \left[ \left( \frac{\rho}{r} \right)^2 + \left( \frac{\rho}{b} \right)^2 \right] \right\} + S \frac{1 + \left( \frac{a}{r} \right)^2}{1 - \left( \frac{a}{b} \right)^2}\end{aligned}\quad (56)$$

For the zone  $c \leq r \leq b$

$$\begin{aligned}\sigma_r &= \frac{\sigma_o}{\sqrt{3}} \left\{ \left[ - \left( \frac{c}{r} \right)^2 + \left( \frac{c}{b} \right)^2 \right] + 2 \left[ \left( \frac{\rho}{r} \right)^2 - \left( \frac{\rho}{b} \right)^2 \right] \right\} + S \frac{1 - \left( \frac{a}{r} \right)^2}{1 - \left( \frac{a}{b} \right)^2} \\ \sigma_\theta &= \frac{\sigma_o}{\sqrt{3}} \left\{ \left[ \left( \frac{c}{r} \right)^2 + \left( \frac{c}{b} \right)^2 \right] - 2 \left[ \left( \frac{\rho}{r} \right)^2 + \left( \frac{\rho}{b} \right)^2 \right] \right\} + S \frac{1 + \left( \frac{a}{r} \right)^2}{1 - \left( \frac{a}{b} \right)^2}\end{aligned}\quad (57)$$

The effect of tensile remote loading is to increase both radial and circumferential stresses. Eventually, when  $S$  becomes sufficiently high, yielding will again occur first from the bore, this time in a positive sense. Using the plain strain yield criterion (7), and (55), the applied stress to initiate yield at the bore is found as

$$S_{o_a} = \frac{2\sigma_o}{\sqrt{3}} \left[ 1 - \left( \frac{a}{b} \right)^2 \right] \quad (58)$$

The magnitude of the remote stress to cause yielding at the bore is thus of the order of the yield stress of the material itself, and this is beyond normal expectation. Practical levels of tensile loading around open cold-worked holes will therefore normally be described by the elastic formulations for stress given above.

The corresponding elastic strains in a coldworked annulus under remote loading are, from (50) to (52) and (15)

For the zone  $a \leq r \leq \rho$

$$\begin{aligned}\epsilon_r &= -\frac{(1+\nu)\sigma_o}{\sqrt{3}E} \left\{ \left( \frac{c}{r} \right)^2 \left[ 1 + (1-2\nu) \left( \frac{c}{b} \right)^2 \right] - 2 \left( \frac{\rho}{r} \right)^2 \left[ 1 + (1-2\nu) \left( \frac{\rho}{b} \right)^2 \right] \right\} \\ &\quad - \frac{S}{E} \left[ \frac{1+\nu}{1 - \left( \frac{a}{b} \right)^2} \right] \left[ \left( \frac{a}{r} \right)^2 - (1-2\nu) \right] \\ \epsilon_\theta &= \frac{(1+\nu)\sigma_o}{\sqrt{3}E} \left\{ \left( \frac{c}{r} \right)^2 \left[ 1 + (1-2\nu) \left( \frac{c}{b} \right)^2 \right] - 2 \left( \frac{\rho}{r} \right)^2 \left[ 1 + (1-2\nu) \left( \frac{\rho}{b} \right)^2 \right] \right\} \\ &\quad + \frac{S}{E} \left[ \frac{1+\nu}{1 - \left( \frac{a}{b} \right)^2} \right] \left[ \left( \frac{a}{r} \right)^2 + (1-2\nu) \right]\end{aligned}\quad (59)$$

For the zone  $\rho \leq r \leq c$

$$\begin{aligned}\epsilon_r &= -\frac{(1+\nu)\sigma_o}{\sqrt{3}E} \left\{ \left(\frac{c}{r}\right)^2 \left[ 1 + (1-2\nu) \left(\frac{c}{b}\right)^2 \right] - 2 \left[ \left(\frac{\rho}{r}\right)^2 - (1-2\nu) \left(\frac{\rho}{b}\right)^2 \right] \right\} \\ &\quad - \frac{S}{E} \left[ \frac{1+\nu}{1-\left(\frac{a}{b}\right)^2} \right] \left[ \left(\frac{a}{r}\right)^2 - (1-2\nu) \right] \\ \epsilon_\theta &= \frac{(1+\nu)\sigma_o}{\sqrt{3}E} \left\{ \left(\frac{c}{r}\right)^2 \left[ 1 + (1-2\nu) \left(\frac{c}{b}\right)^2 \right] - 2 \left[ \left(\frac{\rho}{r}\right)^2 + (1-2\nu) \left(\frac{\rho}{b}\right)^2 \right] \right\} \\ &\quad + \frac{S}{E} \left[ \frac{1+\nu}{1-\left(\frac{a}{b}\right)^2} \right] \left[ \left(\frac{a}{r}\right)^2 + (1-2\nu) \right]\end{aligned}\tag{60}$$

For the zone  $c \leq r \leq b$

$$\begin{aligned}\epsilon_r &= -\frac{(1+\nu)\sigma_o}{\sqrt{3}E} \left\{ \left[ \left(\frac{c}{r}\right)^2 - (1-2\nu) \left(\frac{c}{b}\right)^2 \right] - 2 \left[ \left(\frac{\rho}{r}\right)^2 - (1-2\nu) \left(\frac{\rho}{b}\right)^2 \right] \right\} \\ &\quad - \frac{S}{E} \left[ \frac{1+\nu}{1-\left(\frac{a}{b}\right)^2} \right] \left[ \left(\frac{a}{r}\right)^2 - (1-2\nu) \right] \\ \epsilon_\theta &= \frac{(1+\nu)\sigma_o}{\sqrt{3}E} \left\{ \left[ \left(\frac{c}{r}\right)^2 + (1-2\nu) \left(\frac{c}{b}\right)^2 \right] - 2 \left[ \left(\frac{\rho}{r}\right)^2 + (1-2\nu) \left(\frac{\rho}{b}\right)^2 \right] \right\} \\ &\quad + \frac{S}{E} \left[ \frac{1+\nu}{1-\left(\frac{a}{b}\right)^2} \right] \left[ \left(\frac{a}{r}\right)^2 + (1-2\nu) \right]\end{aligned}\tag{61}$$

The effect on the stress and strain fields of removal of the applied load is readily found by superposition of the elastic equations (10) and (15), but with opposite sign, on the above. For the coldworked annulus example of Section 5, and with an applied stress  $S/\sigma_o = 1/2$ , the stresses for the loaded and unloaded cases are shown in Fig. 11; the strains in Fig. 12. Because all applied loadings result in elastic changes in stress and strain, the 'unloaded' tensile cases are, of course, simply the coldworked residual cases existing prior to remote loading. The cyclic stress and strain regimes occurring under repeated loading are simply those between the loaded and unloaded curves.

### 5.1.2 Compressive Loading ( $S < 0$ )

Compressive remote loading applied to an *open* cold-worked hole introduces entirely different circumstances to those described above. Because the region bordering the hole has already yielded and reyielded, Figs. 8 and 9, the application of remote compressive loading increases the reyielding radius from  $\rho$  to a larger reyield radius  $\tau$ . Upon unloading, superposition of the positive elastic stress field upon the loaded field results in a stress field differing only in mean level from that of the tensile loading case.

For the zone  $a \leq r \leq \tau$  ( $\tau > \rho$ )

In this extended plastic region the stress equations are exactly as for the cold-worked hole alone. Thus, from (47),

$$\begin{aligned}\sigma_r &= -\frac{2\sigma_o}{\sqrt{3}} \ln \frac{\tau}{a} \\ \sigma_\theta &= -\frac{2\sigma_o}{\sqrt{3}} \left[ 1 + \ln \frac{\tau}{a} \right]\end{aligned}\quad (62)$$

It will be seen later that for practical levels of applied remote loading  $\tau$  is certainly within the range  $\rho \leq \tau \leq c$ .

For the zone  $\tau \leq r \leq c$

In this region elastic superposition applies, but with a complication. The extension of the plastic zone modifies the value of  $a$  to be used in the formulation relating to  $S$ . Denoting this new radius by  $\alpha$ , its value is readily found from the requirement of stress continuity across the (new) elasto-plastic boundary  $\tau$ . There results, from (62), (48) and (10), for  $\sigma_r$

$$\begin{aligned}-\frac{2\sigma_o}{\sqrt{3}} \ln \frac{\tau}{a} &= \frac{\sigma_o}{\sqrt{3}} \left\{ \left[ 2 \ln \frac{\tau}{c} - 1 + \left( \frac{c}{b} \right)^2 \right] + 2 \left[ \left( \frac{\rho}{\tau} \right)^2 - \left( \frac{\rho}{b} \right)^2 \right] \right\} \\ &+ S \frac{1 - \left( \frac{\alpha}{\tau} \right)^2}{1 - \left( \frac{\alpha}{b} \right)^2}\end{aligned}\quad (63)$$

and for  $\sigma_\theta$

$$\begin{aligned}-\frac{2\sigma_o}{\sqrt{3}} \left( 1 + \ln \frac{\tau}{a} \right) &= \frac{\sigma_o}{\sqrt{3}} \left\{ \left[ 2 \ln \frac{\tau}{c} + 1 + \left( \frac{c}{b} \right)^2 \right] - 2 \left[ \left( \frac{\rho}{\tau} \right)^2 + \left( \frac{\rho}{b} \right)^2 \right] \right\} \\ &+ S \frac{1 + \left( \frac{\alpha}{\tau} \right)^2}{1 - \left( \frac{\alpha}{b} \right)^2}\end{aligned}\quad (64)$$

Solving (63) and (64) for the unknowns  $\tau$  and  $\alpha$  gives

$$S = -\frac{2\sigma_o}{\sqrt{3}} \left\{ \ln \left( \frac{\tau}{\rho} \right)^2 - \left( \frac{\rho}{b} \right)^2 \left[ \left( \frac{\tau}{\rho} \right)^2 - 1 \right] \right\}\quad (65)$$

and the relationship between elasto-plastic radii as

$$\left(\frac{\alpha}{\tau}\right)^2 = \frac{1 - \left(\frac{\rho}{\tau}\right)^2}{\ln\left(\frac{\tau}{\rho}\right)^2} \quad (66)$$

Thus, for a given compressive remote loading  $S$ ,  $\tau$  is established from (65) and  $\alpha$  from (66).

Substituting (66) into (65) gives a more compact version of the latter as

$$S = -\frac{2\sigma_0}{\sqrt{3}} \left[ \ln\left(\frac{\tau}{\rho}\right)^2 \right] \left[ 1 - \left(\frac{\alpha}{b}\right)^2 \right] \quad (67)$$

Equation (66) is extremely well approximated by

$$\left(\frac{\alpha}{\tau}\right)^2 \simeq \frac{\rho}{\tau} \quad (68)$$

with the approximation becoming exact as  $\rho/\tau \rightarrow 1$ . Rearranging (68) as

$$\alpha \simeq \sqrt{(\rho\tau)} \quad (69)$$

it is seen that  $\alpha$  is given approximately by the geometric mean of the original and the new yield radii.

The stresses in this region are now found by superposition from (10) and (48), after replacing  $a$  by  $\alpha$ , as

$$\begin{aligned} \sigma_r &= \frac{\sigma_0}{\sqrt{3}} \left\{ \left[ 2\ln\frac{r}{c} - 1 + \left(\frac{c}{b}\right)^2 \right] + 2 \left[ \left(\frac{\rho}{r}\right)^2 - \left(\frac{\rho}{b}\right)^2 \right] \right\} + S \frac{1 - \left(\frac{\alpha}{r}\right)^2}{1 - \left(\frac{\alpha}{b}\right)^2} \\ \sigma_\theta &= \frac{\sigma_0}{\sqrt{3}} \left\{ \left[ 2\ln\frac{r}{c} + 1 + \left(\frac{c}{b}\right)^2 \right] - 2 \left[ \left(\frac{\rho}{r}\right)^2 + \left(\frac{\rho}{b}\right)^2 \right] \right\} + S \frac{1 + \left(\frac{\alpha}{r}\right)^2}{1 - \left(\frac{\alpha}{b}\right)^2} \end{aligned} \quad (70)$$

where  $\tau$  is evaluated from (65) and  $\alpha$  from (66).

For the zone  $c \leq r \leq b$

As before, superposition provides the solutions as

$$\begin{aligned}\sigma_r &= \frac{\sigma_o}{\sqrt{3}} \left\{ -\left(\frac{c}{r}\right)^2 + \left(\frac{c}{b}\right)^2 \right\} + 2 \left[ \left(\frac{\rho}{r}\right)^2 - \left(\frac{\rho}{b}\right)^2 \right] \right\} + S \frac{1 - \left(\frac{\alpha}{r}\right)^2}{1 - \left(\frac{\alpha}{b}\right)^2} \\ \sigma_\theta &= \frac{\sigma_o}{\sqrt{3}} \left\{ \left[ \left(\frac{c}{r}\right)^2 + \left(\frac{c}{b}\right)^2 \right] - 2 \left[ \left(\frac{\rho}{r}\right)^2 + \left(\frac{\rho}{b}\right)^2 \right] \right\} + S \frac{1 + \left(\frac{\alpha}{r}\right)^2}{1 - \left(\frac{\alpha}{b}\right)^2}\end{aligned}\quad (71)$$

and  $S < 0$ .

Strains in the elastic regions  $\tau \leq r \leq c$  and  $c \leq r \leq b$  may be written down immediately from (60) and (61) after replacing  $a$  by  $\alpha$ . In the plastic region ( $a \leq r \leq \tau$ ) use is made of the fact that circumferential strain there is proportional to  $1/r^2$ . By equating plastic and elastic  $\epsilon_\theta$  at  $r = \tau$ , the constant of proportionality may be evaluated. Thus,  $\epsilon_\theta$  may be written down and, using (6),  $\epsilon_r$ . The results are

For the zone  $a \leq r \leq \tau$  ( $\tau > \rho$ )

$$\begin{aligned}\epsilon_r &= -\frac{(1+\nu)\sigma_o}{\sqrt{3}E} \left\{ \left(\frac{c}{r}\right)^2 \left[ 1 + (1-2\nu)\left(\frac{c}{b}\right)^2 \right] - 2\left(\frac{\tau}{r}\right)^2 \left[ \left(\frac{\rho}{\tau}\right)^2 + (1-2\nu)\left(\frac{\rho}{b}\right)^2 \right] \right\} \\ &\quad - \frac{S}{E} \left[ \frac{1+\nu}{1 - \left(\frac{\alpha}{b}\right)^2} \right] \left(\frac{\tau}{r}\right)^2 \left[ \left(\frac{\alpha}{\tau}\right)^2 + (1-2\nu) \right]\end{aligned}\quad (72)$$

$$\epsilon_\theta = -\epsilon_r$$

For the zone  $\tau \leq r \leq c$

$$\begin{aligned}\epsilon_r &= -\frac{(1+\nu)\sigma_o}{\sqrt{3}E} \left\{ \left(\frac{c}{r}\right)^2 \left[ 1 + (1-2\nu)\left(\frac{c}{b}\right)^2 \right] - 2 \left[ \left(\frac{\rho}{r}\right)^2 - (1-2\nu)\left(\frac{\rho}{b}\right)^2 \right] \right\} \\ &\quad - \frac{S}{E} \left[ \frac{1+\nu}{1 - \left(\frac{\alpha}{b}\right)^2} \right] \left[ \left(\frac{\alpha}{r}\right)^2 - (1-2\nu) \right] \\ \epsilon_\theta &= \frac{(1+\nu)\sigma_o}{\sqrt{3}E} \left\{ \left(\frac{c}{r}\right)^2 \left[ 1 + (1-2\nu)\left(\frac{c}{b}\right)^2 \right] - 2 \left[ \left(\frac{\rho}{r}\right)^2 + (1-2\nu)\left(\frac{\rho}{b}\right)^2 \right] \right\} \\ &\quad + \frac{S}{E} \left[ \frac{1+\nu}{1 - \left(\frac{\alpha}{b}\right)^2} \right] \left[ \left(\frac{\alpha}{r}\right)^2 + (1-2\nu) \right]\end{aligned}\quad (73)$$

For the zone  $c \leq r \leq b$

$$\begin{aligned}
 \epsilon_r = & -\frac{(1+\nu)\sigma_o}{\sqrt{3}E} \left\{ \left[ \left( \frac{c}{r} \right)^2 - (1-2\nu) \left( \frac{c}{b} \right)^2 \right] - 2 \left[ \left( \frac{\rho}{r} \right)^2 - (1-2\nu) \left( \frac{\rho}{b} \right)^2 \right] \right\} \\
 & - \frac{S}{E} \left[ \frac{1+\nu}{1-\left(\frac{\alpha}{b}\right)^2} \right] \left[ \left( \frac{\alpha}{r} \right)^2 - (1-2\nu) \right] \\
 \epsilon_\theta = & \frac{(1+\nu)\sigma_o}{\sqrt{3}E} \left\{ \left[ \left( \frac{c}{r} \right)^2 + (1-2\nu) \left( \frac{c}{b} \right)^2 \right] - 2 \left[ \left( \frac{\rho}{r} \right)^2 + (1-2\nu) \left( \frac{\rho}{b} \right)^2 \right] \right\} \\
 & + \frac{S}{E} \left[ \frac{1+\nu}{1-\left(\frac{\alpha}{b}\right)^2} \right] \left[ \left( \frac{\alpha}{r} \right)^2 + (1-2\nu) \right]
 \end{aligned} \tag{74}$$

where  $S$  throughout is less than zero.

As for tensile loading, the effect of load removal is found by superposition of the elastic stress and strain equations (10) and (15), with opposite sign, on the above. Unlike the tensile loading case where unloading restores the status quo, here, because of the additional yielding which occurs under compressive loading, the unloaded situation is no longer that of the coldworked hole. For the case previously considered and with an applied load of  $S/\sigma_o = -1/2$ , the stresses and strains are shown in Figs. 11 and 12, along with those for unloading. The increased extent of yielding is clear from Fig. 11 ( $\tau/a = 1.50$ ); its effect on strain is seen in Fig. 12.

As for the tensile loading case, compressive cyclic stresses and strains occurring under repeated loading are indicated by the regimes between the loaded and unloaded curves in Figs. 11 and 12. It is seen that, under either tensile or compressive loading, the stress limits are identical in the region from the bore to the original reyield radius  $\rho$ . Fatigue cracking initiating in the bore and propagating through this region would, therefore, on the basis of stress alone, be independent of the sign of the applied loading. At larger radii, the tensile cyclic stress limits are higher than those for compressive loading, and fatigue crack growth in those regions must proceed more rapidly under cyclic tensile loading. In terms of strain, the circumferential strain limits under tensile loading are higher throughout. From this point of view, the fatigue process must be expected to initiate and progress more rapidly under cyclic tensile loading than under cyclic compressive loading.

Because of the elastic response to repeated loading\*, both stress and strain ranges for tensile and compressive cyclic loading are the same, and they are identical to those for the same loading applied to a plain (non-coldworked) annulus. They are, therefore, also given by the summary Tables 5 and 6.

\* In the case of compressive loading, only after the first half-cycle: see Fig. 12.

## 5.2 Interference Loading

It is assumed in the following that interference is specified relative to the coldworked radius, and not relative to that existing prior to coldworking. This means that, under elastic conditions (normal for interference fitting) the interface pressure between pin and annulus will be the same for a given interference as for a non-coldworked hole. It is given by (23) and, in conjunction with (26) and (27) and (47) to (52) inclusive, the stresses and strains resulting from interference fitting a cold-expanded hole may be written down directly.

For the zone  $a \leq r \leq \rho$

$$\begin{aligned}\sigma_r &= -\frac{2\sigma_o}{\sqrt{3}} \ln \frac{r}{a} - \frac{iE}{D} \left[ \left( \frac{a}{r} \right)^2 - \left( \frac{a}{b} \right)^2 \right] \\ \sigma_\theta &= -\frac{2\sigma_o}{\sqrt{3}} \left[ 1 + \ln \frac{r}{a} \right] + \frac{iE}{D} \left[ \left( \frac{a}{r} \right)^2 + \left( \frac{a}{b} \right)^2 \right]\end{aligned}\quad (75)$$

For the zone  $\rho \leq r \leq c$

$$\begin{aligned}\sigma_r &= \frac{\sigma_o}{\sqrt{3}} \left\{ \left[ 2 \ln \frac{r}{c} - 1 + \left( \frac{c}{b} \right)^2 \right] + 2 \left[ \left( \frac{\rho}{r} \right)^2 - \left( \frac{\rho}{b} \right)^2 \right] \right\} - \frac{iE}{D} \left[ \left( \frac{a}{r} \right)^2 - \left( \frac{a}{b} \right)^2 \right] \\ \sigma_\theta &= \frac{\sigma_o}{\sqrt{3}} \left\{ \left[ 2 \ln \frac{r}{c} + 1 + \left( \frac{c}{b} \right)^2 \right] - 2 \left[ \left( \frac{\rho}{r} \right)^2 + \left( \frac{\rho}{b} \right)^2 \right] \right\} + \frac{iE}{D} \left[ \left( \frac{a}{r} \right)^2 + \left( \frac{a}{b} \right)^2 \right]\end{aligned}\quad (76)$$

For the zone  $c \leq r \leq b$

$$\begin{aligned}\sigma_r &= \frac{\sigma_o}{\sqrt{3}} \left\{ \left[ - \left( \frac{c}{r} \right)^2 + \left( \frac{c}{b} \right)^2 \right] + 2 \left[ \left( \frac{\rho}{r} \right)^2 - \left( \frac{\rho}{b} \right)^2 \right] \right\} - \frac{iE}{D} \left[ \left( \frac{a}{r} \right)^2 - \left( \frac{a}{b} \right)^2 \right] \\ \sigma_\theta &= \frac{\sigma_o}{\sqrt{3}} \left\{ \left[ \left( \frac{c}{r} \right)^2 + \left( \frac{c}{b} \right)^2 \right] - 2 \left[ \left( \frac{\rho}{r} \right)^2 + \left( \frac{\rho}{b} \right)^2 \right] \right\} + \frac{iE}{D} \left[ \left( \frac{a}{r} \right)^2 + \left( \frac{a}{b} \right)^2 \right]\end{aligned}\quad (77)$$

It can be seen that the effect of interference fitting on the stresses resulting from cold expansion is to decrease the radial stress and to increase the circumferential stress. Eventually, a situation will be reached where reyielding will again occur at the bore. By substituting from (75) with  $r = a$  into the yield criterion (7), the degree of interference to cause incipient reyielding at the hole is found as

$$i_o = \frac{2\sigma_o D}{\sqrt{3} E} \quad (78)$$

which is just twice that required to initiate yield in a non-coldworked hole, (29).

The strains in these regions are given by For the zone  $a \leq r \leq \rho$

$$\begin{aligned} \epsilon_r = & -\frac{(1+\nu)\sigma_0}{\sqrt{3}E} \left\{ \left(\frac{c}{r}\right)^2 \left[ 1 + (1-2\nu) \left(\frac{c}{b}\right)^2 \right] - 2 \left(\frac{\rho}{r}\right)^2 \left[ 1 + (1-2\nu) \left(\frac{\rho}{b}\right)^2 \right] \right\} \\ & - \frac{i(1+\nu)}{D} \left[ \left(\frac{a}{r}\right)^2 - (1-2\nu) \left(\frac{a}{b}\right)^2 \right] \end{aligned} \quad (79)$$

$$\begin{aligned} \epsilon_\theta = & \frac{(1+\nu)\sigma_0}{\sqrt{3}E} \left\{ \left(\frac{c}{r}\right)^2 \left[ 1 + (1-2\nu) \left(\frac{c}{b}\right)^2 \right] - 2 \left(\frac{\rho}{r}\right)^2 \left[ 1 + (1-2\nu) \left(\frac{\rho}{b}\right)^2 \right] \right\} \\ & + \frac{i(1+\nu)}{D} \left[ \left(\frac{a}{r}\right)^2 + (1-2\nu) \left(\frac{a}{b}\right)^2 \right] \end{aligned}$$

For the zone  $\rho \leq r \leq c$

$$\begin{aligned} \epsilon_r = & -\frac{(1+\nu)\sigma_0}{\sqrt{3}E} \left\{ \left(\frac{c}{r}\right)^2 \left[ 1 + (1-2\nu) \left(\frac{c}{b}\right)^2 \right] - 2 \left[ \left(\frac{\rho}{r}\right)^2 - (1-2\nu) \left(\frac{\rho}{b}\right)^2 \right] \right\} \\ & - \frac{i(1+\nu)}{D} \left[ \left(\frac{a}{r}\right)^2 - (1-2\nu) \left(\frac{a}{b}\right)^2 \right] \end{aligned} \quad (80)$$

$$\begin{aligned} \epsilon_\theta = & \frac{(1+\nu)\sigma_0}{\sqrt{3}E} \left\{ \left(\frac{c}{r}\right)^2 \left[ 1 + (1-2\nu) \left(\frac{c}{b}\right)^2 \right] - 2 \left[ \left(\frac{\rho}{r}\right)^2 + (1-2\nu) \left(\frac{\rho}{b}\right)^2 \right] \right\} \\ & + \frac{i(1+\nu)}{D} \left[ \left(\frac{a}{r}\right)^2 + (1-2\nu) \left(\frac{a}{b}\right)^2 \right] \end{aligned}$$

For the zone  $c \leq r \leq b$

$$\begin{aligned} \epsilon_r = & -\frac{(1+\nu)\sigma_0}{\sqrt{3}E} \left\{ \left[ \left(\frac{c}{r}\right)^2 - (1-2\nu) \left(\frac{c}{b}\right)^2 \right] - 2 \left[ \left(\frac{\rho}{r}\right)^2 - (1-2\nu) \left(\frac{\rho}{b}\right)^2 \right] \right\} \\ & - \frac{i(1+\nu)}{D} \left[ \left(\frac{a}{r}\right)^2 - (1-2\nu) \left(\frac{a}{b}\right)^2 \right] \end{aligned} \quad (81)$$

$$\begin{aligned} \epsilon_\theta = & \frac{(1+\nu)\sigma_0}{\sqrt{3}E} \left\{ \left[ \left(\frac{c}{r}\right)^2 + (1-2\nu) \left(\frac{c}{b}\right)^2 \right] - 2 \left[ \left(\frac{\rho}{r}\right)^2 + (1-2\nu) \left(\frac{\rho}{b}\right)^2 \right] \right\} \\ & + \frac{i(1+\nu)}{D} \left[ \left(\frac{a}{r}\right)^2 + (1-2\nu) \left(\frac{a}{b}\right)^2 \right] \end{aligned}$$

It is seen that the effect on strains of interference fitting a coldworked hole is to decrease further the radial strain and to increase further the circumferential strain, as expected.

### 5.3 Interference and Remote Loading

In the previous Section it was shown that the effect of interference fitting a cold-expanded hole was to superimpose an elastic stress system which gave rise to no further yielding. The effect of a superimposed remote stress on an interference fitted, cold-expanded hole is similarly found by superposition - at least up to some limit, beyond which further yielding will occur. It turns out that, for practical levels of remote loading (and irrespective of sign), the situation remains fully elastic. Use is made of the results of Section 4.3 and the coldworked results of Section 5 in listing the stress and strain equations.

For the zone  $a \leq r \leq \rho$

From (35) and (47)

$$\begin{aligned}\sigma_r &= -\frac{2\sigma_o}{\sqrt{3}} \ln \frac{r}{a} - \frac{iE}{D} \left[ \left(\frac{a}{r}\right)^2 - \left(\frac{a}{b}\right)^2 \right] \\ &\quad + S \frac{1 - \left(\frac{a}{r}\right)^2}{1 - \left(\frac{a}{b}\right)^2} \left\{ 1 + \frac{2(1-\nu^2)}{D} \left[ \frac{\left(\frac{a}{r}\right)^2 - \left(\frac{a}{b}\right)^2}{1 - \left(\frac{a}{r}\right)^2} \right] \right\} \\ \sigma_\theta &= -\frac{2\sigma_o}{\sqrt{3}} \left( 1 + \ln \frac{r}{a} \right) + \frac{iE}{D} \left[ \left(\frac{a}{r}\right)^2 + \left(\frac{a}{b}\right)^2 \right] \\ &\quad + S \frac{1 + \left(\frac{a}{r}\right)^2}{1 - \left(\frac{a}{b}\right)^2} \left\{ 1 - \frac{2(1-\nu^2)}{D} \left[ \frac{\left(\frac{a}{r}\right)^2 + \left(\frac{a}{b}\right)^2}{1 + \left(\frac{a}{r}\right)^2} \right] \right\}\end{aligned}\tag{82}$$

For the zone  $\rho \leq r \leq c$

From (35) and (48)

$$\begin{aligned}\sigma_r &= \frac{\sigma_o}{\sqrt{3}} \left\{ \left[ 2 \ln \frac{r}{c} - 1 + \left(\frac{c}{b}\right)^2 \right] + 2 \left[ \left(\frac{\rho}{r}\right)^2 - \left(\frac{\rho}{b}\right)^2 \right] \right\} \\ &\quad - \frac{iE}{D} \left[ \left(\frac{a}{r}\right)^2 - \left(\frac{a}{b}\right)^2 \right] + S \frac{1 - \left(\frac{a}{r}\right)^2}{1 - \left(\frac{a}{b}\right)^2} \left\{ 1 + \frac{2(1-\nu^2)}{D} \left[ \frac{\left(\frac{a}{r}\right)^2 - \left(\frac{a}{b}\right)^2}{1 - \left(\frac{a}{r}\right)^2} \right] \right\} \\ \sigma_\theta &= \frac{\sigma_o}{\sqrt{3}} \left\{ \left[ 2 \ln \frac{r}{c} + 1 + \left(\frac{c}{b}\right)^2 \right] - 2 \left[ \left(\frac{\rho}{r}\right)^2 + \left(\frac{\rho}{b}\right)^2 \right] \right\} \\ &\quad + \frac{iE}{D} \left[ \left(\frac{a}{r}\right)^2 + \left(\frac{a}{b}\right)^2 \right] + S \frac{1 + \left(\frac{a}{r}\right)^2}{1 - \left(\frac{a}{b}\right)^2} \left\{ 1 - \frac{2(1-\nu^2)}{D} \left[ \frac{\left(\frac{a}{r}\right)^2 + \left(\frac{a}{b}\right)^2}{1 + \left(\frac{a}{r}\right)^2} \right] \right\}\end{aligned}\tag{83}$$

For the zone  $c \leq r \leq b$

From (35) and (49)

$$\begin{aligned} \sigma_r = & \frac{\sigma_o}{\sqrt{3}} \left\{ \left[ -\left(\frac{c}{r}\right)^2 + \left(\frac{c}{b}\right)^2 \right] + 2 \left[ \left(\frac{\rho}{r}\right)^2 - \left(\frac{\rho}{b}\right)^2 \right] \right\} \\ & - \frac{iE}{D} \left[ \left(\frac{a}{r}\right)^2 - \left(\frac{a}{b}\right)^2 \right] + S \frac{1 - \left(\frac{a}{r}\right)^2}{1 - \left(\frac{a}{b}\right)^2} \left\{ 1 + \frac{2(1-\nu^2)}{D} \left[ \frac{\left(\frac{a}{r}\right)^2 - \left(\frac{a}{b}\right)^2}{1 - \left(\frac{a}{r}\right)^2} \right] \right\} \end{aligned} \quad (84)$$

$$\begin{aligned} \sigma_\theta = & \frac{\sigma_o}{\sqrt{3}} \left\{ \left[ \left(\frac{c}{r}\right)^2 + \left(\frac{c}{b}\right)^2 \right] - 2 \left[ \left(\frac{\rho}{r}\right)^2 + \left(\frac{\rho}{b}\right)^2 \right] \right\} \\ & + \frac{iE}{D} \left[ \left(\frac{a}{r}\right)^2 + \left(\frac{a}{b}\right)^2 \right] + S \frac{1 + \left(\frac{a}{r}\right)^2}{1 - \left(\frac{a}{b}\right)^2} \left\{ 1 - \frac{2(1-\nu^2)}{D} \left[ \frac{\left(\frac{a}{r}\right)^2 + \left(\frac{a}{b}\right)^2}{1 + \left(\frac{a}{r}\right)^2} \right] \right\} \end{aligned}$$

Following the format of Section 4.3, in determining the cyclic circumferential stress range, both explicit interference and cold-working components vanish, leaving

$$\Delta\sigma_\theta = \Delta S \frac{1 + \left(\frac{a}{r}\right)^2}{1 - \left(\frac{a}{b}\right)^2} \left\{ 1 - \frac{2(1-\nu^2)}{D} \left[ \frac{\left(\frac{a}{r}\right)^2 + \left(\frac{a}{b}\right)^2}{1 + \left(\frac{a}{r}\right)^2} \right] \right\} \quad (85)$$

which is identical to (36). Thus, as for the non-coldworked hole case, provided the second term in braces above is less than unity, interference fitting a cold-worked hole gives rise to a cyclic circumferential stress range which is a minimum at the bore.

In the region  $a \leq r \leq \rho$ , the mean circumferential stress under cyclic loading is written down directly from (82) as

$$\begin{aligned} \bar{\sigma}_\theta = & -\frac{2\sigma_o}{\sqrt{3}} \left( 1 + \ln \frac{r}{a} \right) + \frac{iE}{D} \left[ \left(\frac{a}{r}\right)^2 + \left(\frac{a}{b}\right)^2 \right] \\ & + S \frac{1 + \left(\frac{a}{r}\right)^2}{1 - \left(\frac{a}{b}\right)^2} \left\{ 1 - \frac{2(1-\nu^2)}{D} \left[ \frac{\left(\frac{a}{r}\right)^2 + \left(\frac{a}{b}\right)^2}{1 + \left(\frac{a}{r}\right)^2} \right] \right\} \end{aligned} \quad (86)$$

It is seen that the effect of coldworking has been to lower the magnitude of mean circumferential stress by the first term which, in the neighbourhood close to the bore, is substantial and may often exceed the second, interference fitting, term. At some distance from the bore the beneficial effect of coldworking diminishes to the point where the circumferential stresses for the coldworked and non-coldworked hole cases become equal. Equating  $\sigma_\theta$  from (35) and (83), and making use of (54), gives this radius as

$$\ln \frac{r}{\rho} - \ln \frac{\rho}{a} = \left( \frac{\rho}{r} \right)^2 \quad (87)$$

when  $\rho \leq r \leq c$  and, from (35) and (84) as

$$\left( \frac{\rho}{r} \right)^2 = \frac{2 \left( \frac{\rho}{b} \right)^2 - \left( \frac{c}{b} \right)^2}{\left( \frac{c}{\rho} \right)^2 - 2} \quad (88)$$

when  $c \leq r \leq b$ . For the example previously given, where  $\rho = 1.19a$ , this 'crossover' radius occurs at  $r = 2.01a$ .

From (86), the mean circumferential stress at the bore is given by

$$\bar{\sigma}_\theta = -\frac{2\sigma_o}{\sqrt{3}} + \frac{iE}{D} \left[ 1 + \left( \frac{a}{b} \right)^2 \right] + \frac{2\bar{S}}{1 - \left( \frac{a}{b} \right)^2} \left\{ 1 - \frac{1 - \nu^2}{D} \left[ 1 + \left( \frac{a}{b} \right)^2 \right] \right\} \quad (89)$$

which is identical to that for the non-coldworked case (42) apart from the yield term. As already noted, this term is large and, consequently, of substantial fatigue benefit in lowering the magnitude of the circumferential mean stress there.

Thus, the combination of interference fitting (which gives rise to a reduced cycle stress component at the bore) and hole coldworking (which reduces the mean stress at the bore caused by interference fitting) gives rise to a stress system which should benefit fatigue life in the pre-crack and early crack growth stage. This is, of course, the dominant period in terms of total fatigue life.

Strains are found by superposition as follows:

For the zone  $a \leq r \leq \rho$

From (43) and (50)

$$\begin{aligned} \left\{ \begin{matrix} \epsilon_r \\ \epsilon_\theta \end{matrix} \right\} = & \mp \frac{(1+\nu)\sigma_0}{\sqrt{3}E} \left\{ \left( \frac{c}{r} \right)^2 \left[ 1 + (1-2\nu) \left( \frac{c}{b} \right)^2 \right] - 2 \left( \frac{\rho}{r} \right)^2 \left[ 1 + (1-2\nu) \left( \frac{\rho}{b} \right)^2 \right] \right\} \\ & \mp \frac{i(1+\nu)}{D} \left[ \left( \frac{a}{r} \right)^2 \mp (1-2\nu) \left( \frac{a}{b} \right)^2 \right] \mp \frac{S}{E} \left[ \frac{1+\nu}{1-\left(\frac{a}{b}\right)^2} \right] \left[ \left( \frac{a}{r} \right)^2 \mp (1-2\nu) \right] \\ & \times \left\{ 1 - \frac{2(1-\nu^2)}{D} \left[ \frac{\left(\frac{a}{r}\right)^2 \mp (1-2\nu)\left(\frac{a}{b}\right)^2}{\left(\frac{a}{r}\right)^2 \mp (1-2\nu)} \right] \right\} \end{aligned} \quad (90)$$

For the zone  $\rho \leq r \leq c$

From (43) and (51)

$$\begin{aligned} \left\{ \begin{matrix} \epsilon_r \\ \epsilon_\theta \end{matrix} \right\} = & \mp \frac{(1+\nu)\sigma_0}{\sqrt{3}E} \left\{ \left( \frac{c}{r} \right)^2 \left[ 1 + (1-2\nu) \left( \frac{c}{b} \right)^2 \right] - 2 \left[ \left( \frac{\rho}{r} \right)^2 \mp (1-2\nu) \left( \frac{\rho}{b} \right)^2 \right] \right\} \\ & \mp \frac{i(1+\nu)}{D} \left[ \left( \frac{a}{r} \right)^2 \mp (1-2\nu) \left( \frac{a}{b} \right)^2 \right] \mp \frac{S}{E} \left[ \frac{1+\nu}{1-\left(\frac{a}{b}\right)^2} \right] \left[ \left( \frac{a}{r} \right)^2 \mp (1-2\nu) \right] \\ & \times \left\{ 1 - \frac{2(1-\nu^2)}{D} \left[ \frac{\left(\frac{a}{r}\right)^2 \mp (1-2\nu)\left(\frac{a}{b}\right)^2}{\left(\frac{a}{r}\right)^2 \mp (1-2\nu)} \right] \right\} \end{aligned} \quad (91)$$

For the zone  $c \leq r \leq b$

From (43) and (52)

$$\begin{aligned} \left\{ \begin{matrix} \epsilon_r \\ \epsilon_\theta \end{matrix} \right\} = & \mp \frac{(1+\nu)\sigma_0}{\sqrt{3}E} \left\{ \left[ \left( \frac{c}{r} \right)^2 \mp (1-2\nu) \left( \frac{c}{b} \right)^2 \right] - 2 \left[ \left( \frac{\rho}{r} \right)^2 \mp (1-2\nu) \left( \frac{\rho}{b} \right)^2 \right] \right\} \\ & \mp \frac{i(1+\nu)}{D} \left[ \left( \frac{a}{r} \right)^2 \mp (1-2\nu) \left( \frac{a}{b} \right)^2 \right] \mp \frac{S}{E} \left[ \frac{1+\nu}{1-\left(\frac{a}{b}\right)^2} \right] \left[ \left( \frac{a}{r} \right)^2 \mp (1-2\nu) \right] \\ & \times \left\{ 1 - \frac{2(1-\nu^2)}{D} \left[ \frac{\left(\frac{a}{r}\right)^2 \mp (1-2\nu)\left(\frac{a}{b}\right)^2}{\left(\frac{a}{r}\right)^2 \mp (1-2\nu)} \right] \right\} \end{aligned} \quad (92)$$

As for the loading cases for the plain annulus considered in Section 4, all elastic stresses and strains for the loaded cold-worked annulus considered in Section 5 have been grouped together in Tables 7 and 8. Cyclic stress and strain ranges are readily found from (82), (83) and (84), and (90), (91) and (92) by omitting the coldworking and interference terms and replacing  $S$  by  $\Delta S$ . As previously noted, the results for a coldworked annulus are identical to those for a plain annulus: they are listed in Tables 5 and 6.

The incipience of yield at the bore of the interference-fitted, remotely-loaded cold-expanded hole is found by substituting from (82) into the yield criterion (7) and setting  $r = a$ . The results are, for  $S > 0$ ,

$$\frac{S_o}{\sigma_o} = i \frac{E}{\sigma_o} \left[ \frac{1 - \left(\frac{a}{b}\right)^2}{2(1 - \nu^2) - D} \right] \quad (93)$$

and for  $S < 0$

$$\frac{S_o}{\sigma_o} = \left( i \frac{E}{\sigma_o} - \frac{2}{\sqrt{3}} D \right) \left[ \frac{1 - \left(\frac{a}{b}\right)^2}{2(1 - \nu^2) - D} \right] \quad (94)$$

The region between these limits is that in which elastic behaviour occurs. As for the plain hole case of Fig. 7, the elastic regimes for representative cold-expanded cases are shown in Fig. 13. As before, higher positive stress gives rise to separation between pin and hole, the upper limit to elastic behaviour then being governed by that of an open coldworked hole.

As for the non-coldworked hole case, separation, open hole yield and combined loading cases coincide at the point shown, whose co-ordinates are

$$\begin{aligned} \frac{S_o}{\sigma_o} &= \frac{2}{\sqrt{3}} \left[ 1 - \left(\frac{a}{b}\right)^2 \right] \\ i_o &= \frac{4}{\sqrt{3}} \frac{\sigma_o}{E} (1 - \nu^2) \end{aligned} \quad (95)$$

Comparison of (95) with (46) shows that coldworking has extended, by a factor of two, the elastic regime, both stresswise and in terms of interference. This is also readily apparent by comparing Fig. 13 with Fig. 7, both of which are drawn to the same scale.

## 6. CONCLUSIONS

The complete elastic and plastic stress and strain distributions have been presented or derived for an elastic/perfectly-plastic annulus loaded remotely, by interference fitting and with both loadings acting together for both plain and coldworked holes under conditions of plain strain. This study indicates the following:

- (i) Under the action of remote loading, and provided the Young's modulus of the pin is greater than that of the annulus material, interference fitting gives rise to a reduction in cyclic circumferential stress amplitude which is a maximum at the bore: the greater the ratio of Young's moduli, the greater the reduction. For a rigid pin, the factor on circumferential stress range at the bore is about 0.6. This is to be compared with a factor of the order of 2.0 for an open annulus under remote load. Interference fitting itself gives rise to a tensile residual circumferential stress which is a maximum at the bore.
- (ii) Hole coldworking gives rise to a large compressive circumferential stress in the region neighbouring the hole of the order of the yield stress of the annulus material.
- (iii) The combination of interference fitting a coldworked annulus gives rise to a stress system close to the hole in which, under the action of cyclic remote loading, a reduced circumferential stress range operates in conjunction with a compressive mean stress. This stress combination must be very effective in delaying the onset of fatigue cracking and in inhibiting its growth rate when the crack itself is still small.

## REFERENCES

1. Jost, G.S. Stresses and strains in a cold-worked annulus. Dept. Defence, Aeronautical Research Laboratory, Aircraft Structures Report 434, September 1988.
2. Carey, R.P. Three-dimensional computation of stress, strain and strain energy density under interference-fit and after cold-working of holes. Dept. Defence, Aeronautical Research Laboratory, Aircraft Structures Technical Memorandum 478, January 1988.
3. Timoshenko, S. and Goodier, J.N. Theory of Elasticity. McGraw-Hill, Second edition, 1951.
4. Crews, J.H. An elastic analysis of stresses in a uniaxially loaded sheet containing an interference-fit bolt. NASA TN D-6955, October 1972.

Table 1 Cases Considered by Section Number

Geometry	Type of Loading		
	Remote	Interference	Combined
Solid Pin	3.	-	-
Plain Annulus	4.1	4.2	4.3
Coldworked Annulus	5.1	5.2	5.3

Table 2(a) Chosen Parameter Values used in Worked Examples

$$b/a = 5$$

$$c/a = 2.5$$

$$\nu = \nu_p = 1/3$$

$$g = 0, 1/3, 1 \quad (D = 1.778, 1.493, 1.351)$$

$$\sigma_o = 480MPa$$

$$E = 69,000MPa$$

$$S/\sigma_o = \pm 1/2$$

$$i = 0.5\%$$

Table 2(b) Deduced Parameter Values in Worked Examples

$$\rho/a = 1.19$$

$$\alpha/a = 1.34$$

$$\tau/a = 1.50$$

Table 3 Stresses in a Loaded Annulus - Plain Hole

Remote loading only (open hole)

$$\begin{aligned}\sigma_r &= S \frac{1 - \left(\frac{a}{r}\right)^2}{1 - \left(\frac{a}{b}\right)^2} \\ \sigma_\theta &= S \frac{1 + \left(\frac{a}{r}\right)^2}{1 - \left(\frac{a}{b}\right)^2}\end{aligned}\quad (10)$$

Interference only

$$\begin{aligned}\sigma_r &= -\frac{iE}{D} \left[ \left(\frac{a}{r}\right)^2 - \left(\frac{a}{b}\right)^2 \right] \\ \sigma_\theta &= \frac{iE}{D} \left[ \left(\frac{a}{r}\right)^2 + \left(\frac{a}{b}\right)^2 \right]\end{aligned}\quad (26)$$

Combined interference and remote loading\*

$$\begin{aligned}\sigma_r &= -\frac{iE}{D} \left[ \left(\frac{a}{r}\right)^2 - \left(\frac{a}{b}\right)^2 \right] + S \frac{1 - \left(\frac{a}{r}\right)^2}{1 - \left(\frac{a}{b}\right)^2} \left\{ 1 + \frac{2(1 - \nu^2)}{D} \left[ \frac{\left(\frac{a}{r}\right)^2 - \left(\frac{a}{b}\right)^2}{1 - \left(\frac{a}{r}\right)^2} \right] \right\} \\ \sigma_\theta &= \frac{iE}{D} \left[ \left(\frac{a}{r}\right)^2 + \left(\frac{a}{b}\right)^2 \right] + S \frac{1 + \left(\frac{a}{r}\right)^2}{1 - \left(\frac{a}{b}\right)^2} \left\{ 1 - \frac{2(1 - \nu^2)}{D} \left[ \frac{\left(\frac{a}{r}\right)^2 + \left(\frac{a}{b}\right)^2}{1 + \left(\frac{a}{r}\right)^2} \right] \right\}\end{aligned}\quad (35)$$

\* For  $S < S_{sep}$ . If  $S \geq S_{sep}$ , stresses are given by remote loading only case (10).

Table 4 Strains in a Loaded Annulus - Plain Hole

Remote loading only (open hole)

$$\begin{aligned}\epsilon_r &= -\frac{S}{E} \left[ \frac{1+\nu}{1-\left(\frac{a}{b}\right)^2} \right] \left[ \left(\frac{a}{r}\right)^2 - (1-2\nu) \right] \\ \epsilon_\theta &= \frac{S}{E} \left[ \frac{1+\nu}{1-\left(\frac{a}{b}\right)^2} \right] \left[ \left(\frac{a}{r}\right)^2 + (1-2\nu) \right]\end{aligned}\quad (15)$$

Interference only

$$\begin{aligned}\epsilon_r &= -\frac{i}{D} (1+\nu) \left[ \left(\frac{a}{r}\right)^2 - (1-2\nu) \left(\frac{a}{b}\right)^2 \right] \\ \epsilon_\theta &= \frac{i}{D} (1+\nu) \left[ \left(\frac{a}{r}\right)^2 + (1-2\nu) \left(\frac{a}{b}\right)^2 \right]\end{aligned}\quad (27)$$

Combined interference and remote loading\*

$$\begin{aligned}\epsilon_r &= -\frac{i}{D} (1+\nu) \left[ \left(\frac{a}{r}\right)^2 - (1-2\nu) \left(\frac{a}{b}\right)^2 \right] - \frac{S}{E} \left[ \frac{1+\nu}{1-\left(\frac{a}{b}\right)^2} \right] \left[ \left(\frac{a}{r}\right)^2 - (1-2\nu) \right] \\ &\quad \times \left\{ 1 - \frac{2(1-\nu^2)}{D} \frac{\left[ \left(\frac{a}{r}\right)^2 - (1-2\nu) \left(\frac{a}{b}\right)^2 \right]}{\left[ \left(\frac{a}{r}\right)^2 - (1-2\nu) \right]} \right\} \\ \epsilon_\theta &= \frac{i}{D} (1+\nu) \left[ \left(\frac{a}{r}\right)^2 + (1-2\nu) \left(\frac{a}{b}\right)^2 \right] + \frac{S}{E} \left[ \frac{1+\nu}{1-\left(\frac{a}{b}\right)^2} \right] \left[ \left(\frac{a}{r}\right)^2 + (1-2\nu) \right] \\ &\quad \times \left\{ 1 - \frac{2(1-\nu^2)}{D} \frac{\left[ \left(\frac{a}{r}\right)^2 + (1-2\nu) \left(\frac{a}{b}\right)^2 \right]}{\left[ \left(\frac{a}{r}\right)^2 + (1-2\nu) \right]} \right\}\end{aligned}\quad (43)$$

\* For  $S < S_{sep}$ . If  $S \geq S_{sep}$ , strains are given by remote loading only case (15).

Table 5 Circumferential Stress Range in Plain and Coldworked Annuli

Remote loading only (open hole)

$$\Delta\sigma_{\theta} = \Delta S \frac{1 + \left(\frac{a}{r}\right)^2}{1 - \left(\frac{a}{b}\right)^2} \quad (11)$$

Combined interference and remote loading

$$\Delta\sigma_{\theta} = \Delta S \frac{1 + \left(\frac{a}{r}\right)^2}{1 - \left(\frac{a}{b}\right)^2} \left\{ 1 - \frac{2(1 - \nu^2)}{D} \left[ \frac{\left(\frac{a}{r}\right)^2 + \left(\frac{a}{b}\right)^2}{1 + \left(\frac{a}{r}\right)^2} \right] \right\} \quad (36)$$

Table 6 Circumferential Strain Range in Plain and Coldworked Annuli

Remote loading only (open hole)

$$\Delta\epsilon_{\theta} = \frac{S}{E} \left[ \frac{1 + \nu}{1 - \left(\frac{a}{b}\right)^2} \right] \left[ \left(\frac{a}{r}\right)^2 + (1 - 2\nu) \right] \quad (15)$$

Combined interference and remote loading

$$\Delta\epsilon_{\theta} = \frac{i}{D} (1 + \nu) \left[ \left(\frac{a}{r}\right)^2 + (1 - 2\nu) \left(\frac{a}{b}\right)^2 \right] + \frac{S}{E} \left[ \frac{1 + \nu}{1 - \left(\frac{a}{b}\right)^2} \right] \left[ \left(\frac{a}{r}\right)^2 + (1 - 2\nu) \right] \\ \times \left\{ 1 - \frac{2(1 - \nu^2)}{D} \frac{\left[ \left(\frac{a}{r}\right)^2 + (1 - 2\nu) \left(\frac{a}{b}\right)^2 \right]}{\left[ \left(\frac{a}{r}\right)^2 + (1 - 2\nu) \right]} \right\} \quad (43)$$

Table 7 Stresses in a Loaded Annulus - Coldworked Hole -  $a < r < \rho$  only

Coldworked annulus (no loading)

$$\begin{aligned}\sigma_r &= -\frac{2\sigma_o}{\sqrt{3}} \ln \frac{r}{a} \\ \sigma_\theta &= -\frac{2\sigma_o}{\sqrt{3}} \left[ 1 + \ln \frac{r}{a} \right]\end{aligned}\quad (47)$$

Remote loading only (open hole)

(i)  $S > 0$

$$\begin{aligned}\sigma_r &= -\frac{2\sigma_o}{\sqrt{3}} \ln \frac{r}{a} + S \frac{1 - \left(\frac{a}{r}\right)^2}{1 - \left(\frac{a}{b}\right)^2} \\ \sigma_\theta &= -\frac{2\sigma_o}{\sqrt{3}} \left[ 1 + \ln \frac{r}{a} \right] + S \frac{1 + \left(\frac{a}{r}\right)^2}{1 - \left(\frac{a}{b}\right)^2}\end{aligned}\quad (55)$$

(ii)  $S < 0$

$$\begin{aligned}\sigma_r &= -\frac{2\sigma_o}{\sqrt{3}} \ln \frac{r}{a} \\ \sigma_\theta &= -\frac{2\sigma_o}{\sqrt{3}} \left[ 1 + \ln \frac{r}{a} \right]\end{aligned}\quad (62)$$

Interference only

$$\begin{aligned}\sigma_r &= -\frac{2\sigma_o}{\sqrt{3}} \ln \frac{r}{a} - \frac{iE}{D} \left[ \left(\frac{a}{r}\right)^2 - \left(\frac{a}{b}\right)^2 \right] \\ \sigma_\theta &= -\frac{2\sigma_o}{\sqrt{3}} \left[ 1 + \ln \frac{r}{a} \right] + \frac{iE}{D} \left[ \left(\frac{a}{r}\right)^2 + \left(\frac{a}{b}\right)^2 \right]\end{aligned}\quad (75)$$

Combined interference and remote loading\*

$$\begin{aligned}\sigma_r &= -\frac{2\sigma_o}{\sqrt{3}} \ln \frac{r}{a} - \frac{iE}{D} \left[ \left(\frac{a}{r}\right)^2 - \left(\frac{a}{b}\right)^2 \right] \\ &\quad + S \frac{1 - \left(\frac{a}{r}\right)^2}{1 - \left(\frac{a}{b}\right)^2} \left\{ 1 + \frac{2(1 - \nu^2)}{D} \left[ \frac{\left(\frac{a}{r}\right)^2 - \left(\frac{a}{b}\right)^2}{1 - \left(\frac{a}{r}\right)^2} \right] \right\} \\ \sigma_\theta &= -\frac{2\sigma_o}{\sqrt{3}} \left( 1 + \ln \frac{r}{a} \right) + \frac{iE}{D} \left[ \left(\frac{a}{r}\right)^2 + \left(\frac{a}{b}\right)^2 \right] \\ &\quad + S \frac{1 + \left(\frac{a}{r}\right)^2}{1 - \left(\frac{a}{b}\right)^2} \left\{ 1 - \frac{2(1 - \nu^2)}{D} \left[ \frac{\left(\frac{a}{r}\right)^2 + \left(\frac{a}{b}\right)^2}{1 + \left(\frac{a}{r}\right)^2} \right] \right\}\end{aligned}\quad (82)$$

\* Provided  $S < S_{sep}$ . If  $S \geq S_{sep}$ , stresses are given by remote loading only case (55).

Table 8 Strains in a Loaded Annulus - Coldworked Hole -  $a < r < \rho$  only

Coldworked Annulus (no loading)

$$\epsilon_r = -\frac{(1+\nu)\sigma_o}{\sqrt{3}E} \left\{ \left(\frac{c}{r}\right)^2 \left[1 + (1-2\nu)\left(\frac{c}{b}\right)^2\right] - 2\left(\frac{\rho}{r}\right)^2 \left[1 + (1-2\nu)\left(\frac{\rho}{b}\right)^2\right] \right\} \quad (50)$$

$$\epsilon_\theta = -\epsilon_r$$

Remote Loading only (open hole)

(i)  $S > 0$

$$\epsilon_r = -\frac{(1+\nu)\sigma_o}{\sqrt{3}E} \left\{ \left(\frac{c}{r}\right)^2 \left[1 + (1-2\nu)\left(\frac{c}{b}\right)^2\right] - 2\left(\frac{\rho}{r}\right)^2 \left[1 + (1-2\nu)\left(\frac{\rho}{b}\right)^2\right] \right\} - \frac{S}{E} \left[ \frac{1+\nu}{1-\left(\frac{a}{b}\right)^2} \right] \left[ \left(\frac{a}{r}\right)^2 - (1-2\nu) \right] \quad (59)$$

$$\epsilon_\theta = \frac{(1+\nu)\sigma_o}{\sqrt{3}E} \left\{ \left(\frac{c}{r}\right)^2 \left[1 + (1-2\nu)\left(\frac{c}{b}\right)^2\right] - 2\left(\frac{\rho}{r}\right)^2 \left[1 + (1-2\nu)\left(\frac{\rho}{b}\right)^2\right] \right\} + \frac{S}{E} \left[ \frac{1+\nu}{1-\left(\frac{a}{b}\right)^2} \right] \left[ \left(\frac{a}{r}\right)^2 + (1-2\nu) \right]$$

(ii)  $S < 0$

$$\epsilon_r = -\frac{(1+\nu)\sigma_o}{\sqrt{3}E} \left\{ \left(\frac{c}{r}\right)^2 \left[1 + (1-2\nu)\left(\frac{c}{b}\right)^2\right] - 2\left(\frac{\tau}{r}\right)^2 \left[ \left(\frac{\rho}{\tau}\right)^2 + (1-2\nu)\left(\frac{\rho}{b}\right)^2 \right] \right\} - \frac{S}{E} \left[ \frac{1+\nu}{1-\left(\frac{a}{b}\right)^2} \right] \left(\frac{\tau}{r}\right)^2 \left[ \left(\frac{a}{\tau}\right)^2 + (1-2\nu) \right] \quad (72)$$

$$\epsilon_\theta = -\epsilon_r$$

Interference only

$$\epsilon_r = -\frac{(1+\nu)\sigma_o}{\sqrt{3}E} \left\{ \left(\frac{c}{r}\right)^2 \left[1 + (1-2\nu)\left(\frac{c}{b}\right)^2\right] - 2\left(\frac{\rho}{r}\right)^2 \left[1 + (1-2\nu)\left(\frac{\rho}{b}\right)^2\right] \right\} - \frac{i(1+\nu)}{D} \left[ \left(\frac{a}{r}\right)^2 - (1-2\nu)\left(\frac{a}{b}\right)^2 \right] \quad (79)$$

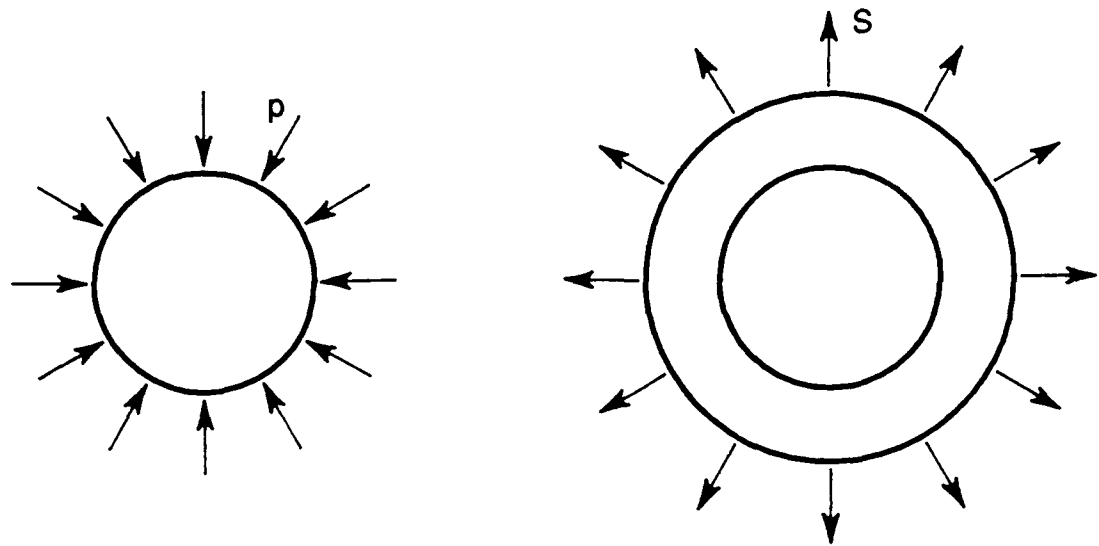
$$\epsilon_\theta = \frac{(1+\nu)\sigma_o}{\sqrt{3}E} \left\{ \left(\frac{c}{r}\right)^2 \left[1 + (1-2\nu)\left(\frac{c}{b}\right)^2\right] - 2\left(\frac{\rho}{r}\right)^2 \left[1 + (1-2\nu)\left(\frac{\rho}{b}\right)^2\right] \right\} + \frac{i(1+\nu)}{D} \left[ \left(\frac{a}{r}\right)^2 + (1-2\nu)\left(\frac{a}{b}\right)^2 \right]$$

Combined interference and remote loading\*

$$\begin{aligned}
 \left\{ \begin{array}{l} \epsilon_r \\ \epsilon_\theta \end{array} \right\} &= \mp \frac{(1+\nu)\sigma_o}{\sqrt{3}E} \left\{ \left(\frac{c}{r}\right)^2 \left[ 1 + (1-2\nu)\left(\frac{c}{b}\right)^2 \right] - 2\left(\frac{\rho}{r}\right)^2 \left[ 1 + (1-2\nu)\left(\frac{\rho}{b}\right)^2 \right] \right\} \\
 &\mp \frac{i(1+\nu)}{D} \left[ \left(\frac{a}{r}\right)^2 \mp (1-2\nu)\left(\frac{a}{b}\right)^2 \right] \mp \frac{S}{E} \left[ \frac{1+\nu}{1-\left(\frac{a}{b}\right)^2} \right] \left[ \left(\frac{a}{r}\right)^2 \mp (1-2\nu) \right] \quad (90) \\
 &\times \left\{ 1 - \frac{2(1-\nu^2)}{D} \left[ \frac{\left(\frac{a}{r}\right)^2 \mp (1-2\nu)\left(\frac{a}{b}\right)^2}{\left(\frac{a}{r}\right)^2 \mp (1-2\nu)} \right] \right\}
 \end{aligned}$$

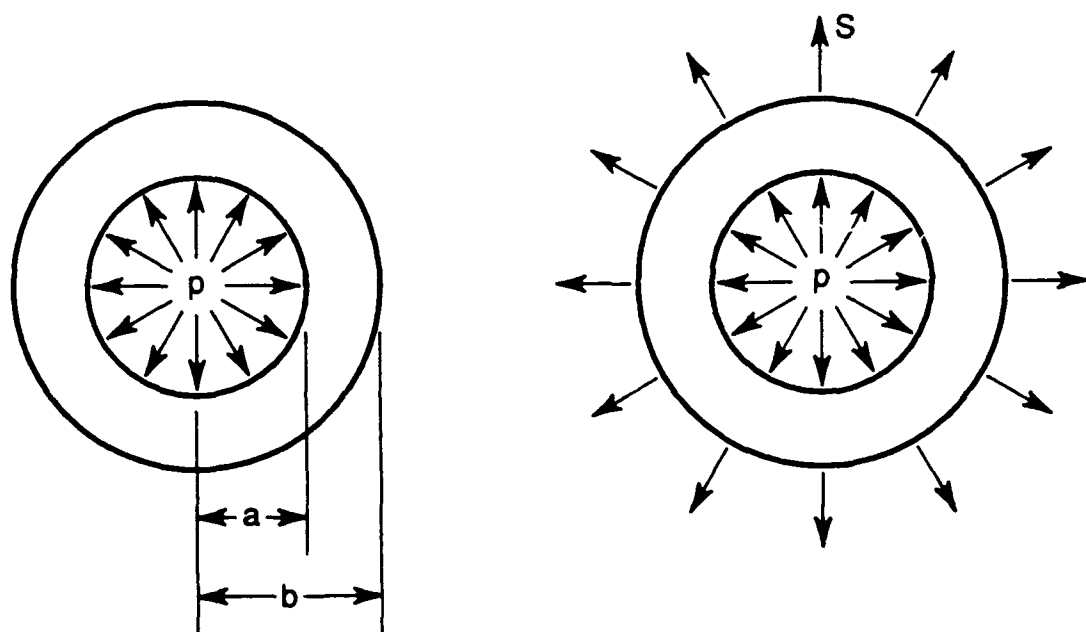
---

\* Provided  $S < S_{sep}$ . If  $S \geq S_{sep}$ , strains are given by remote loading only case (59).



(a) Solid disc

(b) Remote loading



(c) Interference loading

(d) Remote and interference  
(combined) loading

FIGURE 1. LOADING CASES CONSIDERED (CASES b, c AND d WITH AND WITHOUT COLDWORKING)

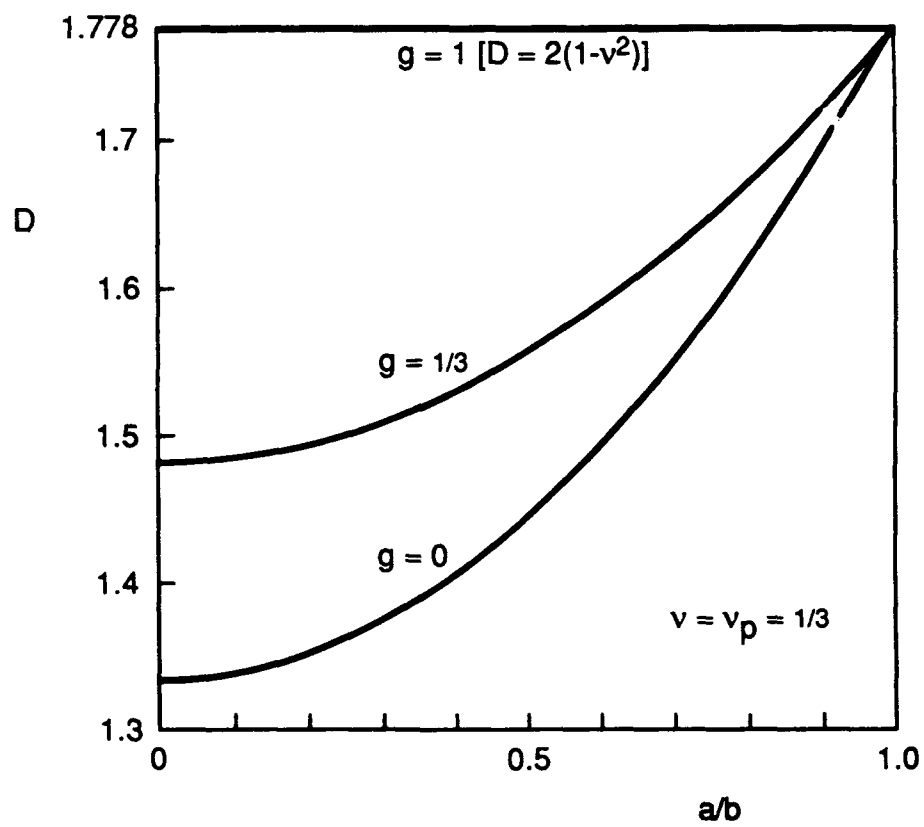


FIGURE 2. EFFECT OF MODULUS RATIO AND GEOMETRY ON D

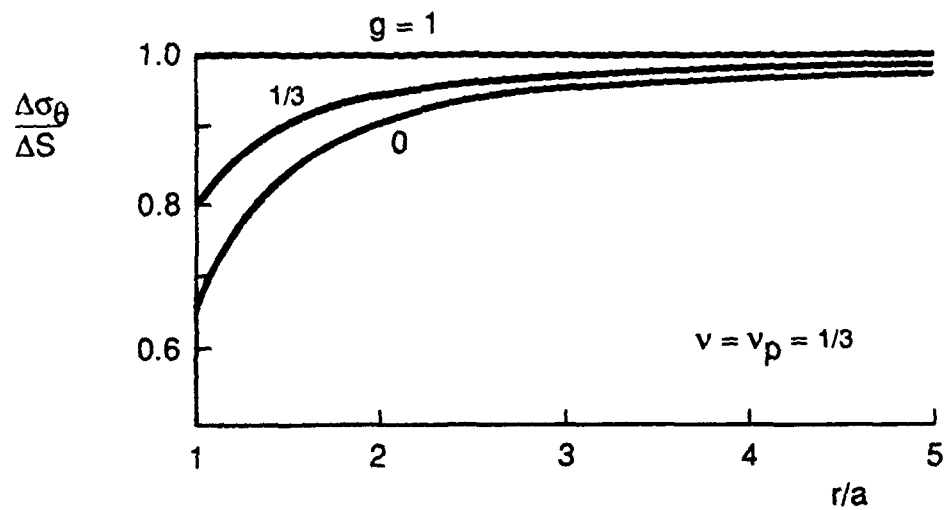


FIGURE 3. CIRCUMFERENTIAL STRESS RANGE FOR COMBINED INTERFERENCE AND REMOTE LOADING: PLAIN AND COLDWORKED HOLES ( $b/a = 5$ )

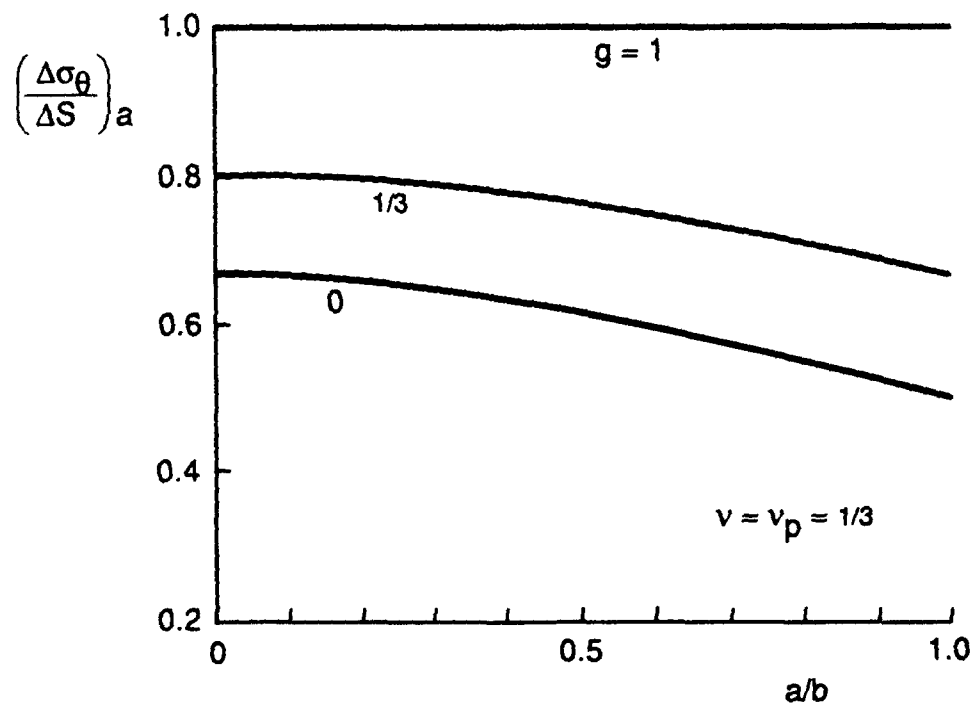


FIGURE 4. EFFECT OF MODULUS RATIO AND GEOMETRY ON CIRCUMFERENTIAL STRESS RANGE AT BORE FOR COMBINED INTERFERENCE AND REMOTE LOADING:

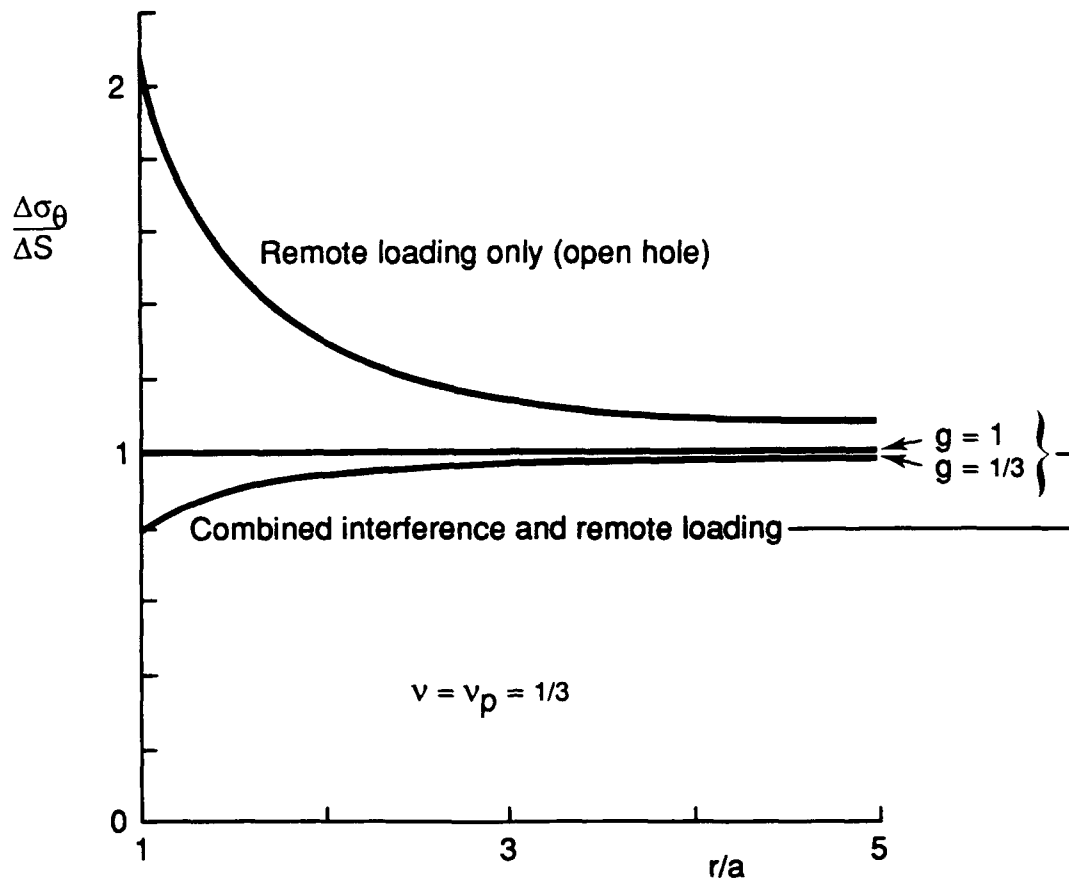


FIGURE 5. EFFECT OF LOADING ON CIRCUMFERENTIAL STRESS RANGE FOR BOTH PLAIN AND COLDWORKED HOLES ( $b/a = 5$ )

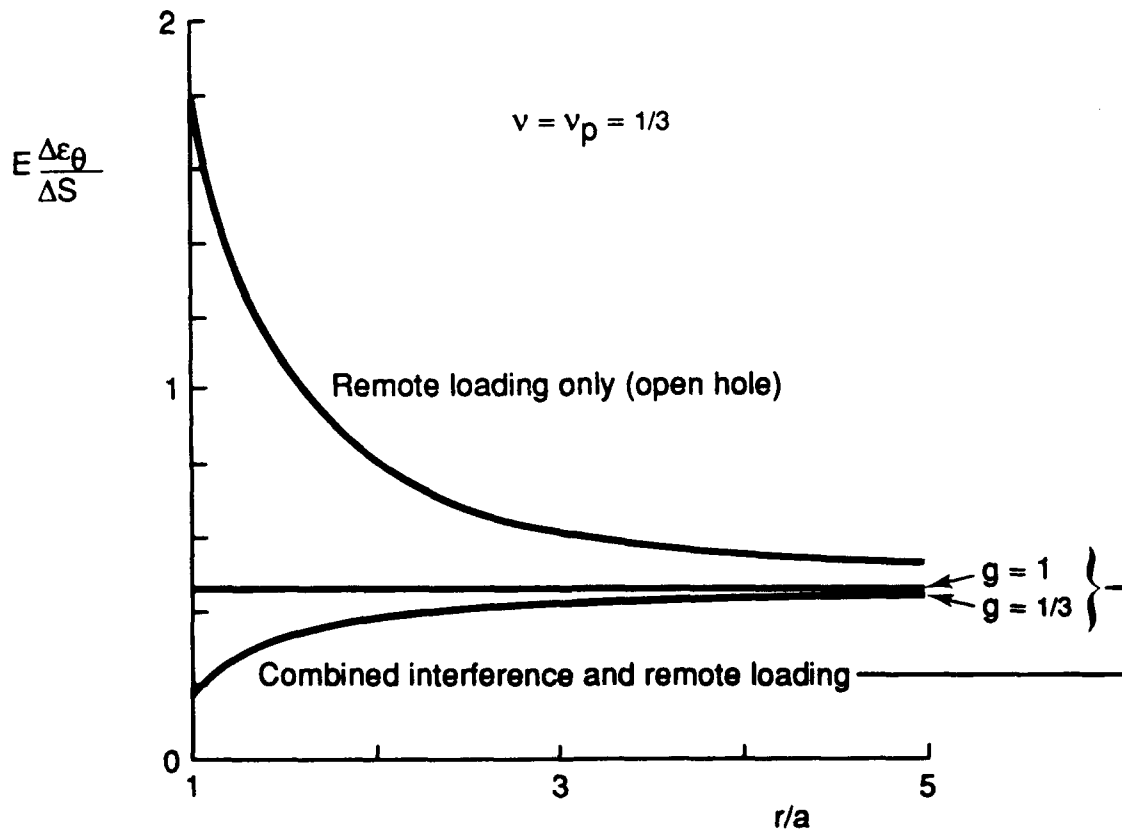


FIGURE 6. EFFECT OF LOADING ON CIRCUMFERENTIAL STRAIN RANGE FOR BOTH PLAIN AND COLDWORKED HOLES ( $b/a = 5$ )

Limits of elastic regime for combined loading ( $g = 1/3$ ) shown shaded

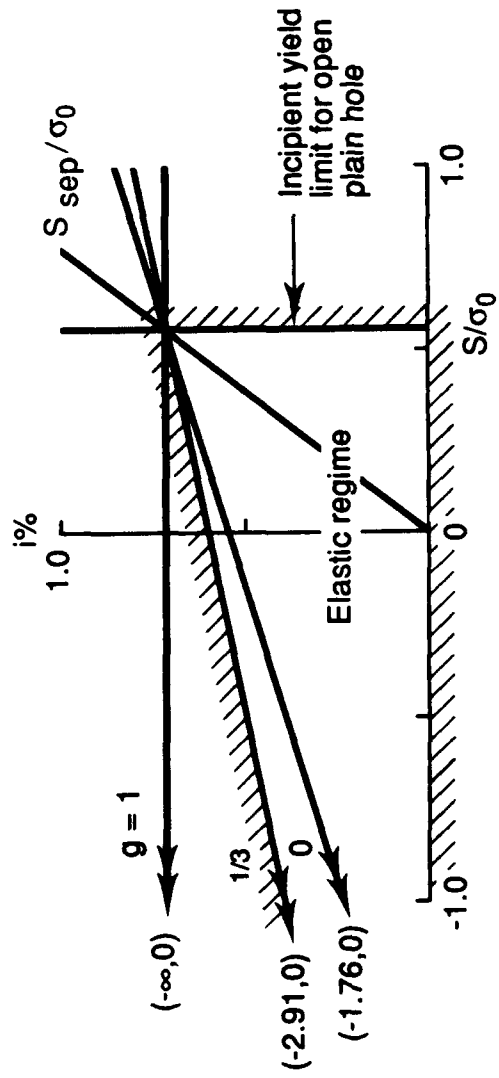
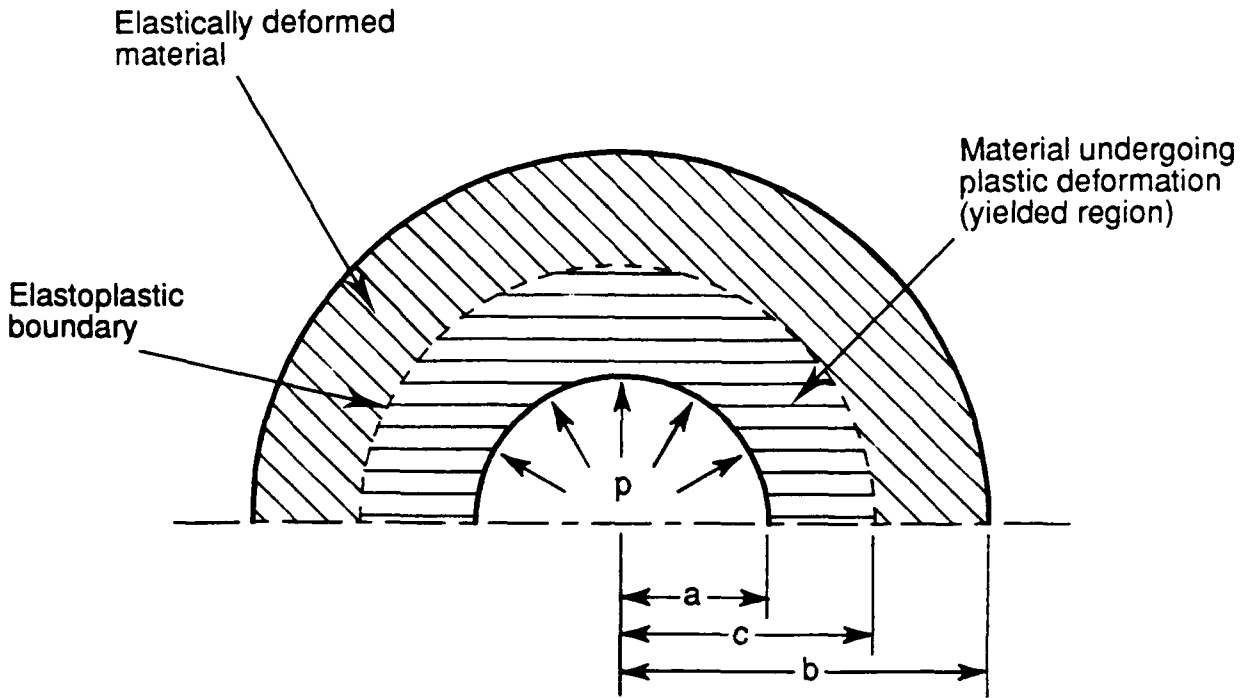
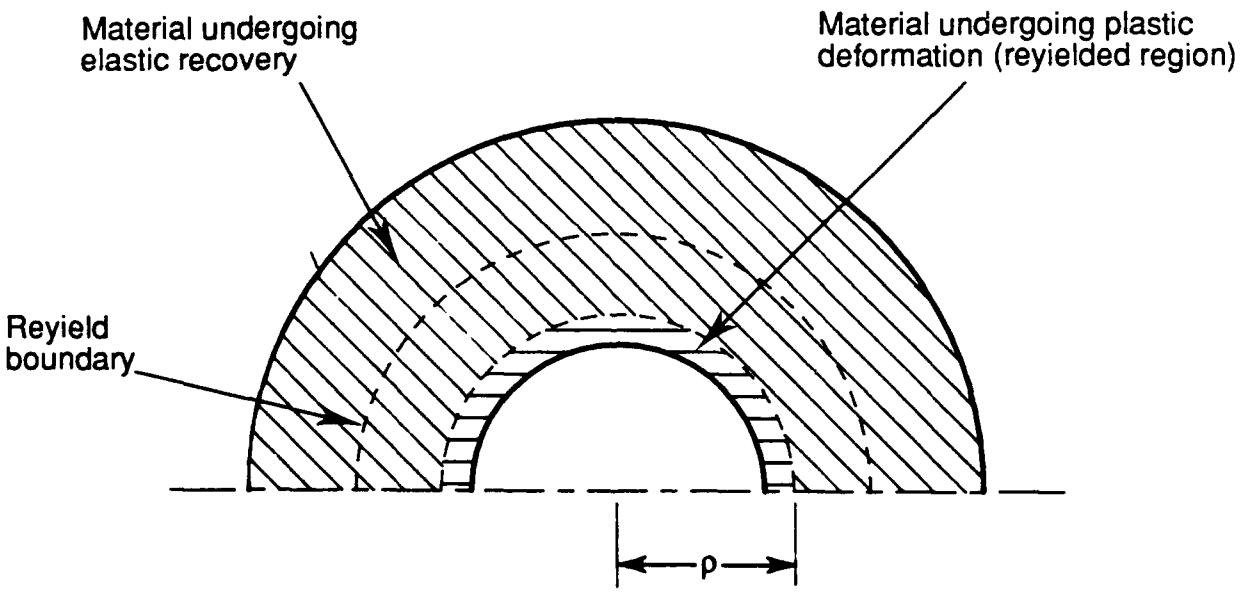


FIGURE 7. ELASTIC REGIMES FOR COMBINED INTERFERENCE FIT AND REMOTE LOADING - PLAIN HOLE ( $b/a = 5$ )



(a) Hole loaded by internal pressure (loaded)



(b) Annulus after removal of internal pressure (unloaded)

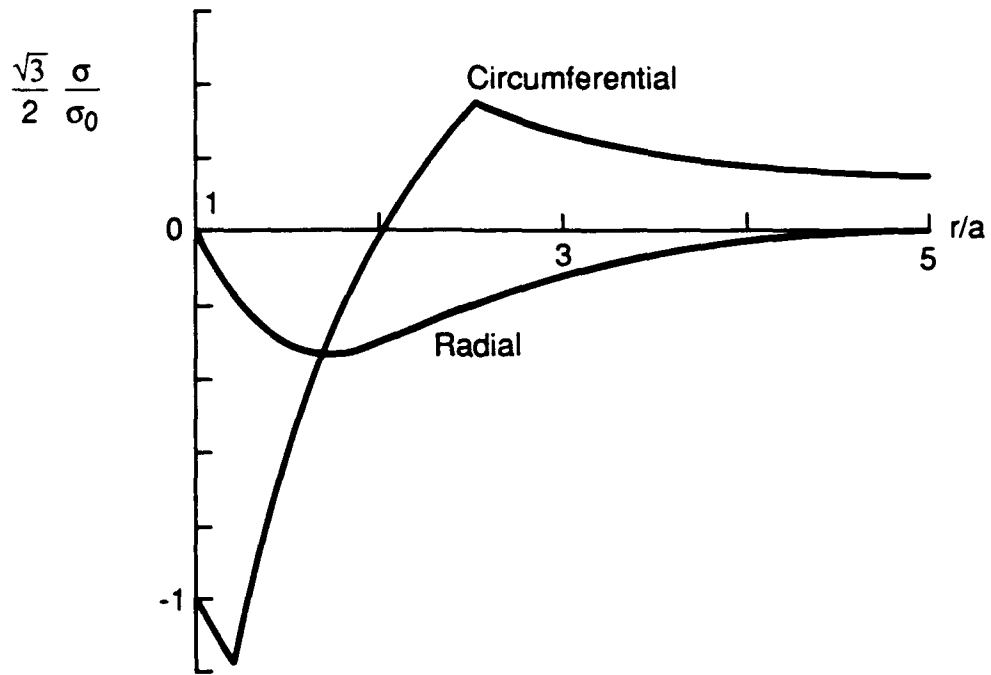
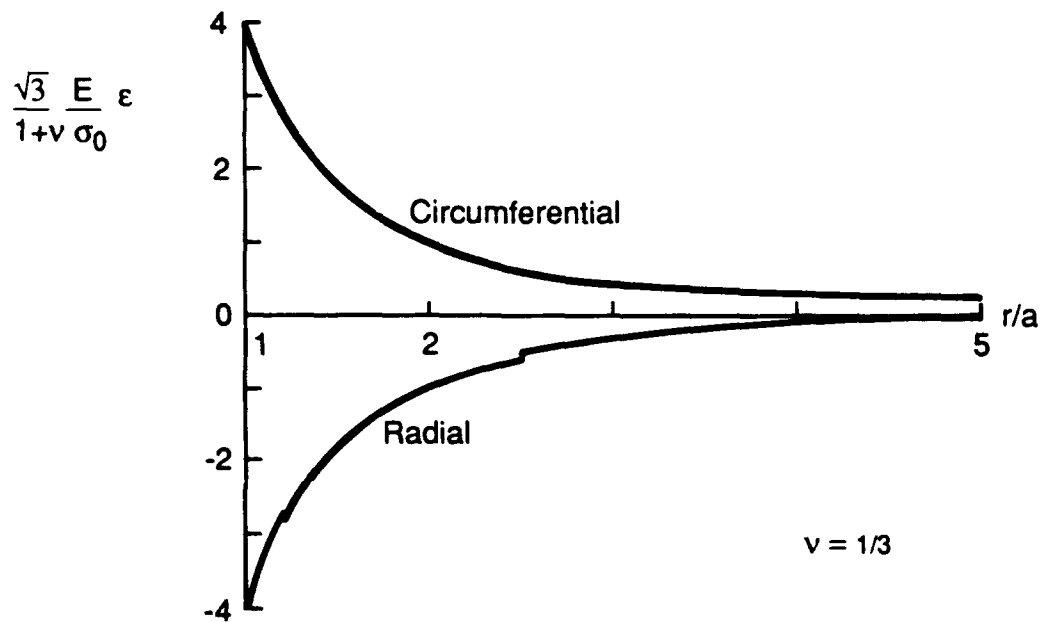


FIGURE 9. RESIDUAL STRESSES IN A COLDWORKED ANNULUS ( $b/a = 5$ )



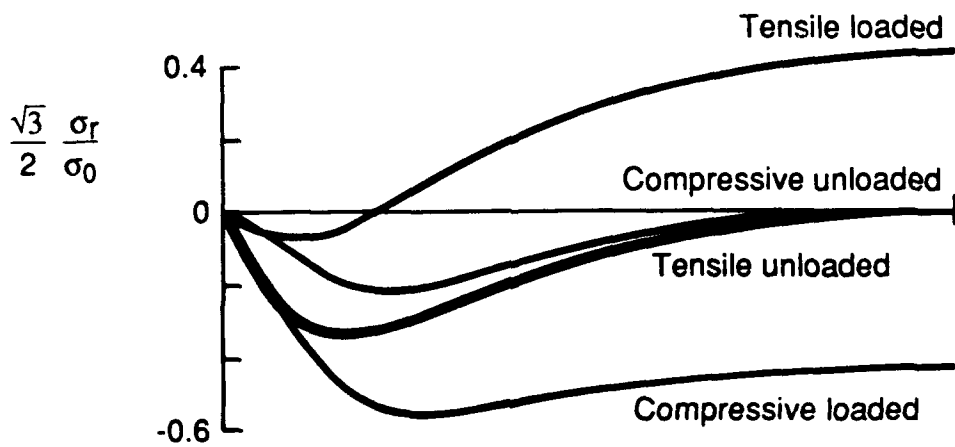
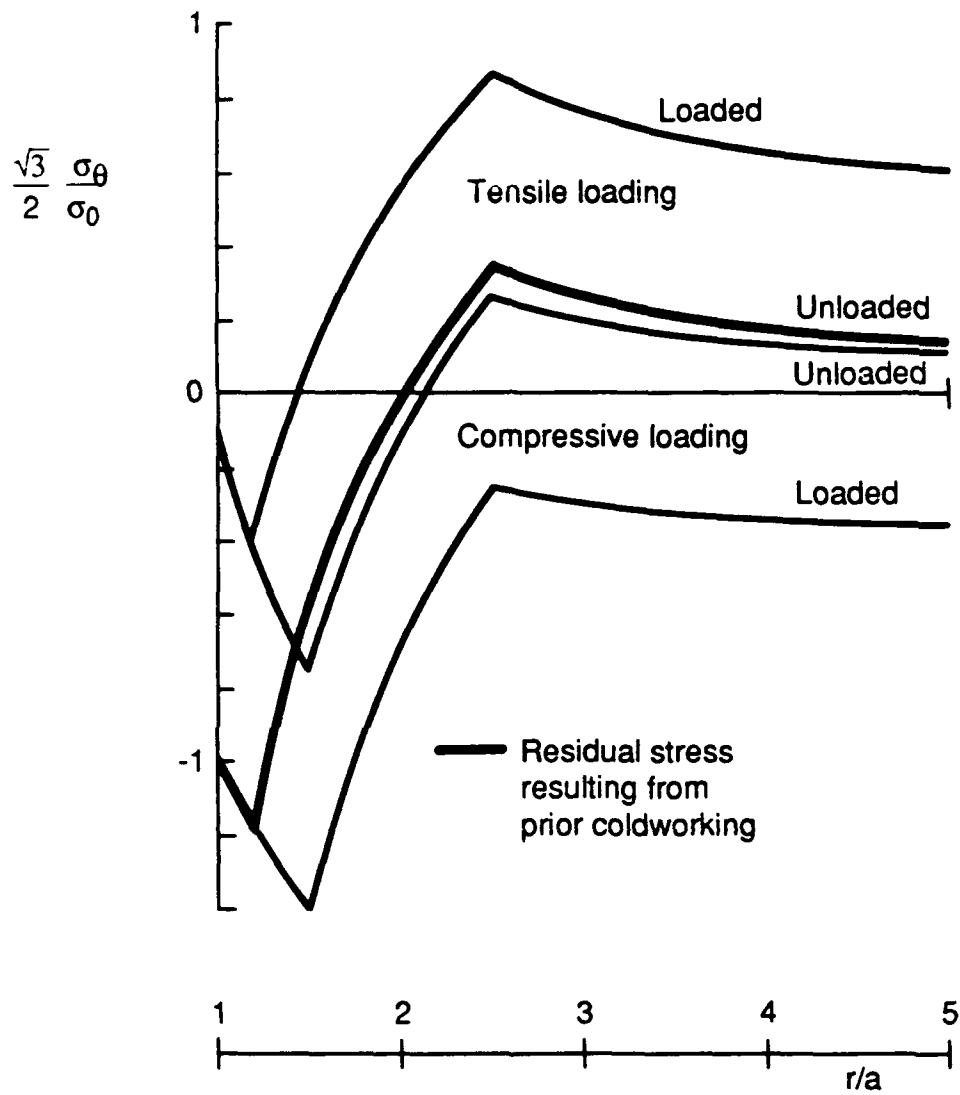


FIGURE 11. STRESSES IN AN OPEN COLDWORKED ANNULUS UNDER TENSILE LOADING ( $S/\sigma_0 = 1/2$ ), COMPRESSIVE LOADING

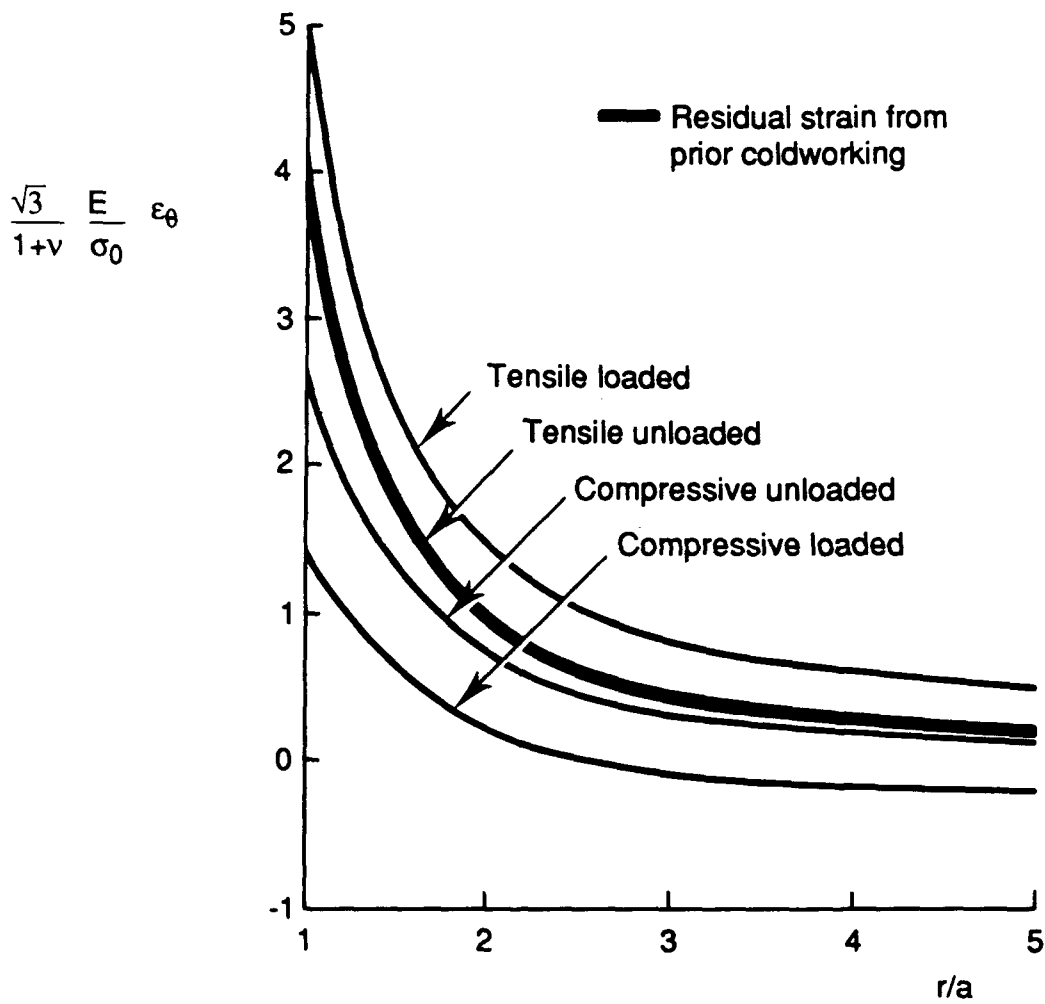


FIGURE 12. CIRCUMFERENTIAL STRAINS IN AN OPEN COLDWORKED ANNULUS UNDER TENSILE LOADING ( $S/\sigma_0 = 1/2$ ), COMPRESSIVE LOADING ( $S/\sigma_0 = -1/2$ ) AND AFTER



## DISTRIBUTION

### AUSTRALIA

#### Department of Defence

##### Defence Central

Chief Defence Scientist )  
AS, Science Corporate Management )shared copy  
FAS Science Policy )  
Director, Departmental Publications  
Counsellor, Defence Science, London (Doc Data sheet only)  
Counsellor, Defence Science, Washington (Doc Data sheet only)  
Scientific Adviser, Defence Central  
OIC TRS, Defence Central Library  
Document Exchange Centre, DSTIC (8 copies)  
Defence Intelligence Organisation  
Librarian H Block, Victoria Barracks, Melb (Doc Data sheet only)

##### Aeronautical Research Laboratory

Director  
Library  
Chief of Structures and Materials Division  
Author: G.S. Jost  
C.K. Rider  
J.M. Finney  
J.G. Sparrow  
R. Jones  
G. Clark  
M. Heller

##### Materials Research Laboratory

Director/Library

##### Defence Science & Technology Organisation - Salisbury

Library

##### Navy Office

Navy Scientific Adviser (3 copies Doc Data sheet only)

##### Army Office

Scientific Adviser - Army (Doc Data sheet only)  
Engineering Development Establishment Library

##### Air Force Office

Air Force Scientific Adviser  
Aircraft Research and Development Unit  
Scientific Flight Group  
Library  
Engineering Branch Library  
HQ Logistics Command (DGELS)

Department of Transport & Communication  
Library

Statutory and State Authorities and Industry

Aero-Space Technologies Australia, Systems Division Librarian  
ASTA Engineering, Document Control Office  
Ansett Airlines of Australia, Library  
Australian Airlines, Library  
Qantas Airways Limited  
Civil Aviation Authority  
Hawker de Havilland Aust Pty Ltd, Victoria, Library  
Hawker de Havilland Aust Pty Ltd, Bankstown, Library

Universities and Colleges

Adelaide

Barr Smith Library  
Professor Mechanical Engineering

Flinders

Library

LaTrobe

Library

Melbourne

Engineering Library

Monash

Hargrave Library

Newcastle

Library

Professor R. Telfer, Institute of Aviation

New England

Library

Sydney

Engineering Library

Dr G.P. Steven, Dept of Aeronautical Engineering

NSW

Physical Sciences Library

Library, Australian Defence Force Academy

Queensland

Library

Tasmania

Engineering Library

Western Australia  
Library

RMIT  
Library  
Mr M.L. Scott, Aerospace Engineering

University College of the Northern Territory  
Library

**CANADA**

CAARC Coordinator Structures  
International Civil Aviation Organization, Library

**NRC**

J.H. Parkin Branch (Aeronautical & Mechanical Engineering Library)  
Division of Mechanical Engineering Library

Universities and Colleges

Toronto  
Institute for Aerospace Studies

**FRANCE**

ONERA, Library  
Mr Raphael Cazes, Dassault Aviation, Division Structures (DGT),

**INDIA**

CAARC Coordinator Structures  
Defence Ministry, Aero Development Establishment Library  
Hindustan Aeronautics Ltd, Library  
National Aeronautical Laboratory, Information Centre

**INTERNATIONAL COMMITTEE ON AERONAUTICAL FATIGUE**

per Australian ICAF Representative (27 copies)

**ISRAEL**

Technion-Israel Institute of Technology  
Roshu Cornell, Dept of Aero Eng., Technion

**JAPAN**

National Aerospace Laboratory  
Institute of Space and Astronautical Science, Library

**NETHERLANDS**

National Aerospace Laboratory (NLR), Library

**NEW ZEALAND**

Defence Scientific Establishment, Library

Universities

Canterbury  
Library

**SINGAPORE**

Director, Defence Materials Organisation

**SWEDEN**

Aeronautical Research Institute, Library

**SWITZERLAND**

F+W (Swiss Federal Aircraft Factory)

**UNITED KINGDOM**

Ministry of Defence, Research, Materials and Collaboration

CAARC, Secretary

Defence Research Agency (Aerospace)

Bedford, Library

Farnborough, Library

National Physical Laboratory, Library

National Engineering Laboratory, Library

British Library, Document Supply Centre

CAARC Coordinator, Structures

Aircraft Research Association, Library

British Aerospace

Kingston-upon-Thames, Library

Hatfield-Chester Division, Library

Short Brothers Ltd, Technical Library

Universities and Colleges

Bristol

Engineering Library

Cambridge

Library, Engineering Department

Whittle Library

London

Head, Aero Engineering

Manchester

Head, Dept of Engineering (Aeronautical)

Nottingham

Science Library

Southampton

Library

Strathclyde

Library

Cranfield Inst. of Technology  
Library

Imperial College  
Aeronautics Library

**UNITED STATES OF AMERICA**

NASA Scientific and Technical Information Facility  
Boeing Commercial Airplanes  
Lockheed-California Company  
Lockheed Georgia  
McDonnell Aircraft Company, Library

Universities and Colleges

Chicago  
John Crerar Library

Florida  
Head, Engineering Sciences

Johns Hopkins  
Head, Engineering Department

Iowa State  
Head, Mechanical Engineering

Princeton  
Head, Mechanics Department

Massachusetts Inst. of Technology  
MIT Libraries

SPARES ( 10 COPIES)

TOTAL (150 COPIES)



PAGE CLASSIFICATION  
UNCLASSIFIED

PRIVACY MARKING

THIS PAGE IS TO BE USED TO RECORD INFORMATION WHICH IS REQUIRED BY THE ESTABLISHMENT FOR ITS OWN USE BUT WHICH WILL NOT BE ADDED TO THE DISTIS DATA UNLESS SPECIFICALLY REQUESTED.

16. ABSTRACT (CONT).

17. IMPRINT

**AERONAUTICAL RESEARCH LABORATORY, MELBOURNE**

18. DOCUMENT SERIES AND NUMBER

Aircraft Structures Report 446

19. COST CODE

25 205A

20. TYPE OF REPORT AND PERIOD COVERED

21. COMPUTER PROGRAMS USED

22. ESTABLISHMENT FILE REF. (S)

23. ADDITIONAL INFORMATION (AS REQUIRED)